Suppression and facilitation of auditory neurons through coordinated acoustic and midbrain stimulation: Investigating a deep brain stimulator for tinnitus

Sarah J. Offutt[1,*], **Kellie J. Ryan**[1], **Alexander E. Konop**[1], and **Hubert H. Lim**[1,2,3]

[1] Department of Biomedical Engineering, University of Minnesota, Minneapolis, USA

[2] Institute for Translational Neuroscience, University of Minnesota, Minneapolis, USA

[3] Department of Otolaryngology, Head and Neck Surgery, University of Minnesota, Minneapolis, USA

Abstract

Objective—The inferior colliculus (IC) is the primary processing center of auditory information in the midbrain and is one site of tinnitus-related activity. One potential option for suppressing the tinnitus percept is through deep brain stimulation via the auditory midbrain implant (AMI), which is designed for hearing restoration and is already being implanted in deaf patients who also have tinnitus. However, to assess the feasibility of AMI stimulation for tinnitus treatment we first need to characterize the functional connectivity within the IC. Previous studies have suggested modulatory projections from the dorsal cortex of the IC (ICD) to the central nucleus of the IC (ICC), though the functional properties of these projections need to be determined.

Approach—In this study, we investigated the effects of electrical stimulation of the ICD on acoustic-driven activity within the ICC in ketamine-anesthetized guinea pigs.

Main Results—We observed ICD stimulation induces both suppressive and facilitatory changes across ICC that can occur immediately during stimulation and remain after stimulation. Additionally, ICD stimulation paired with broadband noise stimulation at a specific delay can induce greater suppressive than facilitatory effects, especially when stimulating in more rostral and medial ICD locations.

Significance—These findings demonstrate that ICD stimulation can induce specific types of plastic changes in ICC activity, which may be relevant for treating tinnitus. By using the AMI with electrode sites positioned within the ICD and ICC, the modulatory effects of ICD stimulation can be tested directly in tinnitus patients.

Keywords

deep brain stimulation; inferior colliculus; tinnitus; hyperacusis; neuromodulation; plasticity

---

***Address correspondence to:** Sarah J. Offutt Department of Biomedical Engineering University of Minnesota 7-105 Nils Hasselmo Hall, 312 Church St SE, Minneapolis, MN 55455 ph: 612-624-7342 fax: (612)-626-6583 offu0004@umn.edu.

Conflict of Interest: None

Introduction

The inferior colliculus (**IC**) is a major convergence center of the auditory system located within the midbrain that integrates bilateral ascending and descending inputs. The IC is subdivided into three main regions: the central nucleus (**ICC**), the external cortex (**ICX**), and the dorsal cortex (**ICD**), each with a distinct role in auditory processing that can be substantiated by the projections to that region (Cant and Benson, 2006; Casseday *et al.*, 2002; Coleman and Clerici, 1987; Faye-Lund and Osen, 1985; Loftus *et al.*, 2010; Oliver, 2005; Roth *et al.*, 1978). The ICC is the best characterized of all the IC regions, comprised of disc-shaped cells arranged in fibrodendritic laminae that constitute the tonotopic area of the IC (Faye-Lund and Osen, 1985; Malmierca *et al.*, 1993; Meininger *et al.*, 1986; Morest and Oliver, 1984; Oliver and Morest, 1984). As the core auditory processing center in the IC, a majority of projections into the ICC ascend from lower auditory centers with a smaller percentage of innervation originating from the auditory cortex (Adams, 1979; Brunso-Bechtold *et al.*, 1981; Oliver *et al.*, 1995; Saint Marie and Baker, 1990; Schofield and Cant, 1996; Shneiderman *et al.*, 1988; Malmierca and Ryugo, 2011; Winer *et al.*, 1998). Unlike the ICC, which is mainly an auditory center, the ICX is innervated by auditory, visual, and somatosensory projections and thus has a role in multi-sensory integration (Aitkin *et al.*, 1978; Aitkin *et al.*, 1981; Binns *et al.*, 1992; Gruters and Groh, 2012; Knudsen, 2002). Questions, however, remain about the role of the ICD in auditory processing.

The role of the ICD in auditory processing may be modulatory, suggested by the extensive inputs the ICD receives descending from the auditory cortex (Faye-Lund, 1985; Herbert *et al.*, 1991; Huffman and Henson, 1990; Winer *et al.*, 1998). Corticofugal projections have been shown to modify frequency tuning and tonotopic maps, shift thresholds, and alter sensitivity to sound localization cues within the ICC (Bajo and King, 2012; Nakamoto *et al.*, 2008; Suga and Ma, 2003; Yan and Suga, 1998; Yan and Ehret, 2002; Zhang *et al.*, 1997). Because the descending projections from primary auditory cortex (**A1**) targeting the ICD are more abundant than those targeting the ICC, it is possible that this descending modulation is achieved, at least in part, by a multi-synaptic pathway to the ICC via the ICD. Anatomical studies within the IC have shown a network of intrinsic projections from the ICD to the ICC that supports this multi-synaptic pathway (Malmierca *et al.*, 1995; Saldaña and Merchán, 1992; Saldana and Merchan, 2005). Modulation via ICD is also implicated by the results of inactivation studies, which have demonstrated changes in the ICC coding properties and plasticity effects when inactivating the IC surface, which likely included the ICD (Jen *et al.*, 2001; Ji *et al.*, 2001; Ji and Suga, 2009). However, there are no studies to our knowledge that have directly activated ICD neurons to confirm and characterize their modulatory effects on ICC neurons.

The effects of ICD stimulation on ICC activity are particularly relevant for recent investigations of a new deep brain stimulator for tinnitus treatment. The auditory midbrain implant (**AMI**) was initially developed for hearing restoration in patients with neurofibromatosis type 2 (**NF2**), a genetic disease that is typically associated with bilateral acoustic neuromas (Colletti *et al.*, 2009; Lenarz *et al.*, 2006; Lim *et al.*, 2009b; Schwartz *et al.*, 2008). These patients become bilaterally deaf due to damage of the auditory nerves inflicted by growth and/or surgical removal of these tumors. For these patients, the AMI

array consisting of one or two shanks with up to 22 electrode sites can be inserted along the tonotopic axis of the ICC with minimal added risks by using the same surgical opening as tumor removal (Lim *et al.*, 2009a; Samii *et al.*, 2007). Due to the hearing loss associated with the tumors, many of these patients also develop tinnitus, which has been linked to changes in spiking activity and synchrony across the auditory system, including the ICC (Bauer *et al.*, 2008; Brozoski *et al.*, 2002; Eggermont and Kenmochi, 1998; Lanting *et al.*, 2009; Ma *et al.*, 2006; Melcher *et al.*, 2009; Møller, 2011; Mulders *et al.*, 2014; Roberts *et al.*, 2010; Vogler *et al.*, 2014; Wang *et al.*, 2011; Zhang and Kaltenbach, 1998).

In the initial AMI clinical trials, three of the five patients had tinnitus. In those three patients, the AMI array was implanted in the ICC, the ICD, and the lateral lemniscus. Stimulation in these patients interfered with the tinnitus percept but did not sufficiently suppress tinnitus (unpublished observations). Considering the proposed modulatory role of ICD, our hypothesis is that appropriate stimulation of ICD may alter auditory neural activity that is effective at suppressing tinnitus. For the one AMI patient implanted in the ICD, complete tinnitus suppression may not have been achieved due to inappropriate placement and stimulation of the electrode sites. Ultimately, we hope the AMI will be able to treat the general tinnitus population and not just deaf individuals undergoing implantation for hearing restoration. For most tinnitus patients who have functional hearing, one exciting opportunity is to combine AMI activation with acoustic stimulation paradigms. There are numerous studies in animals that have demonstrated the immense capability to shift neural coding and induce plasticity within the auditory system by pairing electrical stimulation of modulatory pathways with acoustic stimulation (Engineer *et al.*, 2011; Gao and Suga, 1998; Kilgard and Merzenich, 1998; Suga and Ma, 2003; Weinberger *et al.*, 1993; Xiong *et al.*, 2009). Therefore, we further hypothesize that acoustic stimulation paired with AMI stimulation of different ICD regions could potentially treat tinnitus in humans. Currently, the AMI is designed for stimulating the ICC, but this array can be slightly modified to have electrodes positioned within the ICD. With this modification, we will have the unique opportunity to assess the effects of ICD stimulation on tinnitus perception directly in human patients.

The goal of this study was to investigate the effects of electrical stimulation of the ICD on ascending auditory activity, not only to characterize the modulatory role of the ICD but also to begin assessing the potential for using the AMI for tinnitus treatment. We were primarily interested in determining if differential modulation can be achieved dependent on the ICD stimulation location. In addition, we were interested in the effects of different stimulation paradigms, including electrical stimulation only and electrical stimulation paired with broadband noise stimulation. We initially characterized the changes in acoustic-driven activity within the ICC since anatomical studies have already identified direct connections from the ICD to the ICC. In future studies, we can further assess how ICD stimulation alters neural coding across the auditory system through ascending and descending pathways (Aitkin and Phillips, 1984a; Caicedo and Herbert, 1993; Malmierca and Ryugo, 2011; Winer *et al.*, 1998), especially for properties directly linked to tinnitus. In each animal experiment, we electrically stimulated different regions of the ICD combined with or without broadband noise stimulation. We recorded the corresponding neural changes within different regions of the ICC before, during, and after a given stimulation paradigm to assess immediate and

residual effects. Our results reveal that ICD stimulation induces both suppressive and facilitatory changes throughout the ICC that depend on the location of ICD stimulation as well as its relative timing with acoustic stimulation. These results show that modulation can be achieved through ICD stimulation; whether this modulation is effective in tinnitus treatment can be investigated in future AMI patients.

Methods

Overview

All experiments were performed in ketamine-anesthetized guinea pigs (Elm Hill Labs, Chelmsford, MA) in accordance with the guidelines of the University of Minnesota Institutional Animal Care and Use Committee. Basic surgical and electrophysiological recording and stimulating methods were detailed in previous works (Lim and Anderson, 2007; Markovitz *et al.*, 2012; Straka *et al.*, 2013). Multi-site, silicon-substrate electrode arrays (NeuroNexus Technologies, Ann Arbor, MI) were used to electrically stimulate and record neural activity in the IC. To investigate suppression and facilitation in the ICC during stimulation, multi-unit spike data were recorded in the ICC in response to electrical stimulation of the ICD alone as well as paired with acoustic stimulation at specific inter-stimulus intervals. Additionally, responses to acoustic stimulation alone were recorded before and after each ICD stimulation paradigm to evaluate changes in activity remaining in the ICC after stimulation.

Surgery

Experiments were performed on 12 Hartley guinea pigs (393 ± 50g, Elm Hill, Chelmsford, MA). Animals were initially anesthetized with an intramuscular injection of ketamine (40 mg/kg) and xylazine (10 mg/kg). Anesthesia was administered throughout the experiment to maintain an areflexive state. A warm water blanket was used to maintain a body temperature of 38.0 ± 0.5°C, which was monitored with a rectal thermometer. Additionally, atropine sulfate (0.05 mg/kg) was administered periodically to keep the airway clear of mucous secretion. Animals were positioned in a stereotaxic frame (David Kopf Instruments, Tujunga, CA) using hollow ear bars into the ear canals and a bite bar. A craniotomy was performed to expose the right occipital lobe.

Stimulation and data acquisition

Experiments were performed in an electrically and acoustically isolated sound chamber. Stimulation delivery and data collection were controlled by TDT hardware (Tucker-Davis Technologies, Alachua, FL) and custom software written in MATLAB (MathWorks, Natick, MA). Acoustic stimulation was delivered to the left ear by a speaker coupled to the hollow ear bar at a sampling frequency of 195 kHz. The speaker and ear bar were calibrated using a 0.25-in condenser microphone (ACO Pacific, Belmont, CA). Electrical stimulation was delivered through an optically isolated stimulator. A monopolar configuration was used for both electrical stimulation and recording, with the returns through needle electrodes placed directly into the parietal lobe and in the neck muscle, respectively. Neural signals were passed through analog DC-blocking and anti-aliasing filters from 1.6 Hz to 7.5 kHz and sampled at 24 kHz.

Electrode array placement

Upon removing the dura, micromanipulators (Kopf Instruments, Tujunga, CA) were used to insert arrays into the ICC and the ICD. The electrode arrays consisted of two shanks separated by 500 μm with 16 sites linearly spaced along each shank at a separation of 100 μm. The recording electrode array was inserted at a 45° angle to the sagittal plane and through the occipital cortex into the midbrain to a depth that spans the tonotopic axis in the ICC (Malmierca *et al.*, 1995; Snyder *et al.*, 2004). The stimulating electrode array was inserted at a 90° angle to the horizontal plane and through the occipital cortex to a depth corresponding to the ICD. Some lateral locations corresponding to the ICX may have been included in the analysis, however excluding those points would not have changed our main findings (see data in the *Results*).

To identify the IC during placement of the electrode arrays, broadband noise (50 ms duration, 0.5 ms rise/fall time, 6 octave bandwidth from 0.625 to 40 kHz, 70 dB-SPL) was delivered to the left ear to elicit acoustic-driven responses within the IC. Frequency response maps (**FRMs**), which indicate tuning properties of neurons, were created by presenting a random sequence of pure tones (1-40 kHz, 8 steps per octave) at varying levels (0-70 dB-SPL, 10 dB-SPL steps) with 4 trials presented for each stimulus at 2/s. These FRMs were used to differentiate sites within the ICC versus those within the ICD. Sites in the ICC exhibited a tonotopic gradient from high frequencies on the deepest locations to low frequencies on more shallow sites (Malmierca *et al.*, 2008; Merzenich and Reid, 1974; Snyder *et al.*, 2004). The FRMs of sites in the ICD lacked a tonotopic organization and were predominantly double-peaked or broad in shape with no clear frequency selectivity (LeBeau *et al.*, 2001; Palmer *et al.*, 2013). Prior to placement, electrode arrays were stained with a red fluorescent dye (**Di-I**: 1, 1-dioctadecyl-3,3,3',3'-tetramethylindocarbocyanine perchlorate; Sigma-Aldrich, St Louis, MO) in order to enable identification of the array placements across the IC during the histological analysis.

In some experiments (n=5 animals), a single stimulation array placement was made in the ICD and multiple recording array placements were made in the ICC, as shown in figure 1(a). In the other experiments (n=7 animals), a single recording array placement was made in the ICC and multiple stimulating array placements were made in the ICD, as shown in figure 1(b). Across all 12 experiments, recording placements were made throughout the ICC, shown in the 3D reconstruction in figure 1(c), that fully sampled the ICC along the isofrequency dimension. Figure 1(e) shows a comparison of the recording locations across the ICC from this study to recording locations outside of the ICC taken from a separate mapping study (unpublished data from our lab). Sites designated as outside of the ICC were identified by the lack of systematic tonotopic shifts along the recording shank and fully encapsulate our recording locations (Straka *et al.*, 2014). The stimulating array placements from all 12 experiments are shown in the 3D reconstruction in figure 1(d) and along a 2D plane perpendicular to the array shanks in figure 1(f). Most of the ICD was sampled; however it was not possible to sample the most medial portions of the ICD due to obstructive vasculature on the occipital cortex surface. For experiments where one ICD stimulation array placement and multiple ICC recording array placements are made, analysis was done for each of the ICC sites. Across the 12 experiments, where there are different

numbers of ICD and ICC sites stimulated and recorded dependent on the experimental design used, modulation of each ICD-ICC site pair was analyzed.

Stimulation parameters

Different acoustic and electrical stimulation paradigms were used to examine both suppression and facilitation of neural activity in the ICC. Acoustic stimulation (**AS-only**) consisted of broadband noise stimulation (90 ms duration, 0.5 ms rise/fall time, 6 octave bandwidth from 0.625 to 40 kHz). The level presented varied based on the hearing threshold of each animal, with a typical level delivered at 10 to 20 dB-SPL above the neural threshold such that at least 50% of the ICC sites showed activity significantly above the spontaneous level (see *Methods: Data analysis* for further details). The acoustic stimulation level ranged from 30-70 dB-SPL with an average level across experiments of 40 dB-SPL.

Electrical stimulation consisted of 100 µA biphasic, charge balanced, cathodic leading pulses (205 µs/phase) presented to the ICD. The largest current level safe for the electrode (Lim and Anderson, 2006) was used to elicit the greatest modulation. Due to the limited time per experiment, additional current levels were not tested, though future studies can investigate varying electrical and acoustic levels. Electrical stimulation paradigms included electrical-only stimulation (**ES-only**) and paired acoustic-electrical stimulation. For the paired acoustic-electrical paradigms, the electrical pulse was delivered 8 ms or 18 ms following the onset of acoustic stimulation. The 8 ms paired acoustic-electrical paradigm (**PAES-8**) allowed electrical stimulation to effect the ICC approximately before or simultaneous with the onset of acoustic activation. Onset latencies for acoustic-driven activity within the IC typically range between 4 and 25 ms with an average found for guinea pigs of about 13 ms (Langner *et al.*, 1987; Schreiner and Langner, 1988; Syka *et al.*, 2000; Ter-Mikaelian *et al.*, 2007). The 18 ms paired acoustic-electrical paradigm (**PAES-18**) allowed electrical stimulation to effect the ICC approximately after the onset of acoustic activation.

For each ICD array placement, 3-4 stimulating sites were selected from each shank located within the ICD. The following paradigms were completed sequentially for each stimulating site: AS-only, ES-only, AS-only, PAES-18, AS-only, PAES-8, AS-only. Each paradigm consisted of 100 trials presented at 2 trials/s. All 100 trials were presented for each paradigm before starting the subsequent paradigm. For each stimulating site, the AS-only paradigm was interleaved with electrical paradigms in order to assess different modulatory effects. All seven stimulation paradigms were completed for each stimulation site before proceeding to the next stimulation site. For these experiments, there were many parameters that could have been varied, each potentially affecting the results in different ways. Due to the limited time per experiment and in order to systematically track these potential effects across a reasonable number of animals, we initially chose to focus on varying electrode array placements in the ICC and in the ICD to test the effects of location. In doing so, we used the same acoustic and electrical levels, paradigm order, and recovery time across experiments to minimize their confounding influences on the location effects. In part, we chose this protocol because keeping the locations in the ICC and ICD constant across experiments was not readily possible whereas randomizing locations while keeping the other parameters

constant was. Furthermore, identifying locations for implanting an array in patients will be critical for tinnitus treatment. The ramifications of this methodology in interpreting the results will be discussed in *Discussion: Stimulus timing dependent plasticity*.

Data analysis

The neural recordings were bandpass filtered offline from 0.3 to 3 kHz to extract and analyze multi-unit spike activity. For recordings taken during electrical stimulation, the artifact was removed prior to bandpass filtering the signal. Spikes were counted if the amplitude exceeded three standard deviations above the background noise level. Modulation of ICC activity was only analyzed on sites where acoustic-driven activity was significantly greater than spontaneous activity using signal detection theory (Green and Swets, 1966; Lim and Anderson, 2007), which compared the spike distributions of 90 ms windows of acoustic-driven and spontaneous activity. Sites were excluded if the two distributions of spike counts per trial were not significantly different from each other (d'<1), which was deemed as insufficient evoked neural activity.

Immediate and residual modulation—A two-tailed, unequal variance, ranked t-test (Ruxton, 2006) was used to compare spike count distributions to determine if a recording site underwent immediate or residual modulation, with significance determined at p<0.01. **Immediate** modulation occurred when the spike count distribution for a paired acoustic-electrical stimulation paradigm was significantly different than that for the preceding AS-only paradigm. For all immediate comparisons, spike counts were found within a window which began 4 ms after the onset of the electrical artifact (i.e., immediately after the electrical artifact removal window) and ended at the offset of acoustic stimulation, giving total window lengths of 68 ms for PAES-18 and 78 ms for PAES-8. **Residual** modulation compared the two AS-only spike count distributions surrounding an electrical paradigm. The window for this analysis started 8 ms after the onset of acoustic stimulation to allow for sound transmission to the ICC and ended at the offset of acoustic stimulation for a total window of 82 ms.

Immediate suppression (facilitation) occurred if the activity to paired acoustic-electrical stimulation was significantly lower (higher) than that of the AS-only response preceding the paired paradigm. Immediate modulation was only assessed in comparison to the activity elicited from the preceding AS-only and not to the activity elicited from the preceding ES-only (e.g., to assess the amount of enhancement beyond the sum of the individual paradigms). This approach was selected because there was a relatively small number of ICD-ICC site pairs that exhibited activity in response to ES-only (513 of 4109 ICD-ICC site pairs), which would have limited our ability to perform a summation analysis. Furthermore, the immediate modulation elicited for this group of ICD-ICC site pairs was distributed, with suppression for 101 site pairs, facilitation for 155 site pairs, and no significant change for 257 site pairs, indicating that the presence of activity to ES-only did not always result in facilitation or enhancement. For these reasons, the immediate modulation analysis only focused on how much ICD stimulation could alter ongoing acoustic-driven activity (i.e., ascending coding properties). Residual suppression (facilitation) occurred if the AS-only

response following the electrical paradigm yielded a significantly lower (higher) spike count than the AS-only response preceding the electrical paradigm.

Modulation spread and strength—Two metrics were used to quantify the extent of modulation within the ICC caused by ICD stimulation. The first metric was **spread**, which was the percent of sites across the ICC that were significantly suppressed or facilitated for each ICD stimulation location. The second metric was **strength**, which measured the amount of change that occurred on each of the significantly modulated sites. Strength was calculated as a normalized value by dividing the spike count during the electrical paradigm (for immediate) or the following AS-only paradigm (for residual) by the spike count of the preceding AS-only paradigm.

Histology and maps—The histological process and 3D reconstruction were detailed in a previous publication (Markovitz *et al.*, 2012) and are briefly described here. At the end of an experiment, the animal was euthanized with an intracardial injection of an overdose of pentobarbital. The head was removed and placed in 3.7% paraformaldehyde. The brain was completely removed from the skull within four days following the acute experiment and the right midbrain was sectioned and placed in sucrose within ten days of the acute experiment. After 24 hours in sucrose, the tissue was cryosliced into 60 μm thick slices and mounted on slides. The slices were then imaged and digitally processed to create a 3D midbrain reconstruction using Rhinoceros software (Seattle, WA). A brightfield image was taken of each slice to digitally trace its outline and to align all the slice tracings together into a 3D reconstruction of the midbrain. The positions of the electrode arrays within the 3D midbrain were reconstructed from images taken under a green fluorescent filter, which captured the Di-I stains of the arrays within the brain slices. Once the 3D brain reconstructions were completed for each animal, they were normalized across animals so that all recording and stimulation shanks were superimposed onto one normalized midbrain, as shown in figure 1.

Additional steps were taken to create 2D maps from the 3D renderings that would be used for assessing location trends across the ICC or the ICD for spread and strength. For the ICC, 2D planes were constructed to approximately align with the isofrequency laminae (i.e., orthogonal to the recording arrays; an example plane is shown in figure 1(c)). Planes were created at three different depths relative to the IC surface corresponding to specific laminae in guinea pigs (unpublished data from our lab: 1.3 mm for 3-4.5 kHz, 1.6 mm for 6-9.1 kHz, 1.9 mm for 10-15.2 kHz). The frequency ranges of these laminae were based on the best frequencies (**BFs**) of the recorded sites at those corresponding depths. The BF was calculated from the FRM of each site by taking the frequency centroid of activity at 10 dB-SPL above the minimum threshold, as further described in (Lim and Anderson, 2006). We selected these three frequency ranges, that each spanned two critical bandwidths, because there were a sufficient number of sites for assessing locations trends along these ICC laminae (n=86 for 3-4.5 kHz, n=189 for 6-9.1 kHz, n=158 for 10-15.2 kHz). It is important to note that while the different laminae exhibit some variations in shape and curvature relative to the 45° tonotopic orientation (Malmierca *et al.*, 1995), an approximation of each lamina as a flat plane does not compromise the ability to identify location trends. The

absolute distance between sites may be skewed by the projection onto a flat plane, but the relative locations of sites to each other are preserved.

For analyzing the ICD location effects, the medial-lateral and caudal-rostral coordinates for all stimulating shanks were compiled onto one normalized midbrain reconstruction and mapped onto a single transverse plane, as shown in figures 1(d) and (f). We initially attempted to analyze ICD location effects along the dorsal-to-ventral axis, but further analysis was not pursued as no obvious trend was observed across this dimension. By using a single transverse plane, each shank position only appears as a single point in figure 1(f) even though there can be up to four stimulation sites corresponding to that location. For analyzing stimulation location trends across this single plane, we slightly staggered the locations of all the sites for each shank location so that they could be visible and included in the analysis (e.g., see figure 7).

Results

We analyzed and compared the immediate and residual effects across the ICC for stimulation of different ICD sites for PAES-18, PAES-8, and ES-only to examine modulation differences due to recording and stimulation locations as well as stimulation paradigms. Separate maps for the effects elicited during and after each stimulation paradigm were created in the ICC and the ICD. For the ICC, the strength of the modulation was mapped onto each recording site. For the ICD, the spread produced across ICC by each ICD stimulation site was mapped onto each site location. We did not observe any noticeable location trends across the ICC or the ICD for immediate effects for any of the stimulation paradigms. However, we did observe stimulation location trends across the ICD for residual effects using PAES-18, but not PAES-8 or ES-only. Considering these findings, only the residual data for PAES-18 is presented below. However, a summary of the differences in residual spread resulting from the three stimulation paradigms and a comparison of residual and immediate simulation effects for PAES-18 are included to highlight the unique modulation properties caused by PAES-18.

Residual modulation in the ICC

Neural activity was recorded across the ICC in response to 154 different stimulation sites in the ICD. Stimulation of every ICD site modulated activity in the ICC, though the spread and strength of the suppression or facilitation varied across sites. To obtain a representative measure of spread across the ICC for a stimulated ICD site, we initially analyzed data from experiments in which we mapped multiple shank locations across the ICC (i.e., >34 ICC sites recorded for a given ICD stimulation site). These data correspond to 35 ICD sites from 5 animals. Figures 2(a) and (b) present data from a single animal to show how stimulation of two different ICD sites with PAES-18 can result in varying spread of suppressive activity across the ICC. Stimulation of one site resulted in large suppression spread (figure 2(a), 46.0% of ICC sites suppressed) while stimulation of a second site that was separated by 500 μm resulted in minimal suppression spread (figure 2(b), 11.1%). Differences in spread across ICD sites can also be seen for facilitation in figure 3 in which stimulation of one ICD site resulted in large facilitation spread (figure 3(a), 23.4%) while stimulation of another site

from the same animal resulted in minimal facilitation spread (figure 3(b), 4.7%). For the 35 stimulated ICD sites, histograms of the suppression spread (figure 2(c)) and facilitation spread (figure 3(c)) indicate that stimulation of the ICD generally causes greater residual suppression (mean: 18.2%, SD: 9.5%) than facilitation (mean:6.1%, SD: 6.5%). Significance was determined at $p<0.01$ two-tailed, unequal variance, ranked t-test.

In addition to spread effects, the strength of modulation varied across different ICC recording sites. In figure 4(a), PSTHs of AS-only recordings before and after stimulation are plotted for two different ICC recording sites in response to the same stimulated ICD site. For this example, different suppression strengths were observed for the two ICC sites (decrease of 51.4% versus 13.9%). Figure 4(b) plots the histogram of different suppression strengths across all ICC recording sites in which there was an average decrease of 17.1%. Differences in facilitation strength were also observed across ICC sites. Figure 5(a) shows one example in which different facilitation strengths were observed for two different ICC sites in response to the same stimulated ICD site (increase of 66.5% versus 17.7%). Figure 5(b) plots the histogram of different facilitation strengths across all ICC recordings sites in which there was an average increase of 19.7%. We did not observe any significant differences in the distribution of suppressive and facilitatory strengths, which is evident when comparing figures 4(b) and 5(b). Overall, stimulation of each ICD site resulted in weak and strong modulation of different ICC sites, but there were generally more sites being suppressed than facilitated using PAES-18.

Residual modulation trends across the ICC recording locations

To assess if ICD modulation varied for different recording locations across the ICC laminae, we assembled the data into three different isofrequency planes, as explained in the *Methods: Histology and maps* and shown in figure 6. Each site in figure 6 represents where the shank intersected with the isofrequency plane. On some shanks, multiple recording sites had BFs within each frequency range (low frequency, $n_{shanks}=29$, $n_{sites}=86$; middle frequency, $n_{shanks}=47$, $n_{sites}=189$; high frequency, $n_{shanks}=44$, $n_{sites}=158$). For each shank, a binary analysis was performed to indicate whether or not sites in each frequency range could be significantly modulated by any stimulated ICD site. The filled circles represent locations in ICC that were modulated and unfilled circles represent unmodulated locations. For the low frequency lamina, 58.6% of locations were suppressed and 44.8% were facilitated. For the middle frequency lamina, 91.5% of the locations were suppressed and 68.1% were facilitated. For the high frequency lamina, 75.0% of the locations were suppressed and 52.3% were facilitated. Visual inspection of the binary analysis shown in figure 6 reveals that suppression and facilitation can occur throughout an ICC lamina without any specific regions exhibiting greater modulation. To further evaluate if differential modulation occurred across the ICC, maps of strength were plotted as a function of ICC location (data not shown). No clear location trends were observed across the ICC laminae, consistent with the binary spread plots in figure 6.

Residual modulation trends across the ICD stimulation locations

We mapped all of the ICD site locations onto a 2D plane as shown in figure 7(a). Across 12 animals, 154 different stimulation sites were used from 45 total shank placements for a total

of 4109 ICD-ICC site pairs. Note that each shank placement could have 3-4 ICD sites along the shank, in which we slightly staggered those sites so they could be visualized and analyzed. In figure 7(a), two parameters of spread are mapped for each ICD location. The first is the percent of ICC sites suppressed, represented by the color of the circles, with darker colors indicating larger spread. The second parameter is the maximum number of ICC sites for a given ICD location in which larger circles indicate more sites could have been suppressed in the ICC. Large-dark circles represent ICD sites that elicited a large amount of spread in comparison to large-light circles that represent ICD sites that had the potential to suppress a large number of ICC sites but failed to do so. Since we visually observed a location trend in figure 7(a), we further analyzed the ICD map to define the steepest gradient axis for spread, which corresponds to a vector across ICD showing the direction of the greatest change in suppression spread. The steepest gradient axis was calculated by two-dimensional multiple linear regression analysis where the modulation response was predicted by the location of each stimulation site. Figure 7(b) shows that the spread of suppression significantly increases as a function of ICD location along that steepest gradient axis ($p \ll 0.001$; along the dotted black line in figure 7(a)). The weakest spread of suppression occurred from stimulation of sites in the caudal-lateral region of the ICD. Similar plots and analyses were performed for facilitation spread. As shown in figure 8, no clear location trend was observed across the ICD and we did not identify any significant steepest gradient axis for facilitation spread (data not shown). Our findings indicate that the greater spread of suppression versus facilitation for PAES-18 is due to ICD stimulation location rather than ICC recording location. In particular, PAES-18 causes greater suppression in ICC when stimulating in more rostral and medial ICD locations, while eliciting facilitation in ICC when stimulating throughout the ICD.

Differences in residual spread across stimulation paradigms

In contrast to PAES-18, we did not observe any location trends for ES-only and PAES-8. Figure 9 summarizes the differences in spread effects for these three stimulation paradigms, using only the data from experiments in which we mapped multiple shank locations across the ICC. The spread of suppression for PAES-18 is significantly larger than that of the other two paradigms ($18.2 \pm 9.7\%$ compared to $12.9 \pm 8.9\%$ for ES-only, $p < 0.05$, and $12.5 \pm 12.1\%$ for PAES-8, $p < 0.05$). Conversely, the facilitation spread is significantly reduced for PAES-18 compared to the other two paradigms ($6.1 \pm 6.5\%$ compared to $9.9 \pm 6.9\%$ for ES-only, $p < 0.05$, and $9.6 \pm 5.9\%$ for PAES-8, $p < 0.05$). In comparing suppression versus facilitation effects, figure 9 indicates that paired stimulation with a specific delay (i.e., PAES-18; $p \ll 0.001$) can cause different extents of suppressive versus facilitatory modulation that does not occur for another delay (i.e., PAES-8) or ES-only.

Immediate modulation guides residual modulation

In addition to the residual analysis described above, we also analyzed and compared the immediate changes in the ICC caused by PAES-18 and by PAES-8. Sites could be modulated immediately and/or residually or show no change due to paired stimulation, as shown in table 1. From the results of PAES-18 and PAES-8, a total of 705 ICD-ICC site pairs (8.8%) were both immediately and residually modulated significantly across all experiments. For each of these site pairs, the strength of the immediate modulation and of

the residual modulation were plotted and compared in figure 10. Of all the ICD-ICC site pairs modulated immediately and residually by a paired paradigm, 66.2% of sites that were immediately suppressed were also residually suppressed and 25.0% of sites that were immediately facilitated were also residually facilitated. These results suggest that the type of modulation (i.e., suppression or facilitation) that occurs during PAES-18 or PAES-8 drives the type of residual modulation for sites that are both immediately and residually modulated. Only 8.8% of sites switched modulation direction following stimulation.

Discussion

The goals of these experiments were to identify the types of ICC modulation possible through electrical stimulation of the ICD, to determine if any location trends existed in either the ICC or the ICD, and to compare the extent of suppression and facilitation elicited in ICC by different ICD stimulation paradigms. For all three electrical stimulation paradigms, we observed both immediate and residual suppression and facilitation across different ICC locations. We also observed that stimulation of every location in the ICD caused some amount of significant modulation in neural activity in the ICC. In particular, each ICD site could modulate a different subset of ICC neurons (<40% of the ICD-ICC sites pairs shown in table 1 with varied patterns shown in figure 2 and figure 3). For PAES-18, more residual spread of suppression was elicited by stimulating rostral and medial regions of the ICD. Compared to PAES-8 and ES-only, PAES-18 also appeared to exhibit significantly more residual spread of suppression and less residual spread of facilitation, suggesting that paired stimulation with different inter-stimulus delays can alter the relative amount of suppression versus facilitation across the ICC. Furthermore, the type of residual modulation was predicted by the type of immediate modulation. In a majority of ICD-ICC site pairs that were both immediately and residually modulated, sites that were immediately suppressed (facilitated) were also residually suppressed (facilitated). In summary, our findings demonstrate that ICD stimulation can modulate the ICC and that targeting different ICD regions with paired acoustic-electrical stimulation may be a way to induce varying types of plasticity within the ascending auditory pathway, which in turn could potentially modulate the tinnitus percept.

Functional connectivity between the ICD and the ICC

Our results show that stimulation of the ICD both increases and decreases spiking activity in the ICC, which is in contrast to the functional effects shown from the ICX to the ICC that were found to be inhibitory (Jen *et al.*, 2001; Jen *et al.*, 2002). Previous studies have shown that corticofugal activation and inactivation of the ICC can lead to excitatory and inhibitory changes within the ICC (Mitani *et al.*, 1983; Sun *et al.*, 1989; Syka and Popelar, 1984; Torterolo *et al.*, 1998; Zhang and Suga, 2000; Zhou and Jen, 2000). Considering that projections from auditory cortex to the IC, including the ICC, are considered to be excitatory (i.e., glutamatergic; (Feliciano and Potashner, 1995; Rockel and Jones, 1973; Saint Marie, 1996; Saldana *et al.*, 1996), it is expected that inhibitory effects within the ICC are induced by the auditory cortex through a multi-synaptic pathway via the ICD and the ICX. Corticofugal excitatory effects, especially for frequency specific changes in the ICC, are expected to involve both direct projections to the ICC (Bajo and Moore, 2005; Bajo *et al.*,

2007; Lim and Anderson, 2007; Markovitz *et al.*, 2013; Saldana *et al.*, 1996; Xiong *et al.*, 2009; Yan and Suga, 1999) and indirect multi-synaptic projections via the ICD. Our results support this type of functional organization, which is also consistent with the excitatory and inhibitory synapses from the ICD to the ICC shown in previous anatomical studies (González-Hernández *et al.*, 1996; Nakamoto *et al.*, 2013; Saint Marie, 1996).

Methodological considerations in interpreting location trends

There are several potential limitations to consider when interpreting our results. The first set of limitations relates to the ICD location trends observed in our study. Location trends could have been affected by the limited recovery time allowed by our chosen experimental protocol. The modulatory effects elicited by one stimulation site may have lasted for tens of minutes to several hours, and thus influenced or masked the modulatory effects of proceeding stimulation sites. However, we specifically designed our experimental protocol to minimize this issue, wherein the ICD stimulation locations were varied within an experiment and across all experiments by starting in different locations and moving to sites in different directions. Therefore, if a location trend was observed (i.e., for residual spread of suppression following PAES-18), then we know it truly exists. If a trend was not observed (i.e., for residual spread of facilitation following PAES-18 or other possible trends), then it may still exist but was somehow masked by our protocol.

ICD location trends may have also been missed due to the artificial way electrical stimulation activates central neurons. In using monopolar electrical stimulation, which can cause current spread out to hundreds of microns depending on the cell type and orientation (McIntyre and Grill, 2000; Ranck, 1975), we could have stimulated a complex network of neurons as well as overlapping populations across different ICD sites. Additionally, electrical stimulation may have activated axons passing by the stimulated sites that originate within or outside of ICD. One example of passing fibers include commissural projections, which arise from every subregion in the IC and project to homotopic regions of the contralateral IC (Aitkin and Phillips, 1984b; Coleman and Clerici, 1987; González Hernández *et al.*, 1986; Malmierca *et al.*, 1995; Saldaña and Merchán, 1992). These commissural projections are both glutamatergic and GABAergic (González-Hernández *et al.*, 1996; Saint Marie, 1996; Hernández *et al.*, 2006) and have induced both excitatory and inhibitory effects on neurons in the contralateral IC in functional electrical stimulation and pharmacology experiments (Malmierca *et al.*, 2003; Malmierca *et al.*, 2005; Moore *et al.*, 1998; Smith, 1992), similar to the effect seen in the data presented here. Therefore, it is possible that the suppressive and facilitatory effects we observed in the ICC in response to ICD stimulation could be caused, in part, by activation of commissural neurons. Clinically, it is not an issue if we are activating a larger area of ICD including neurons within as well as passing fibers through ICD as long as electrical stimulation of the corresponding implant location in ICD in humans can sufficiently modulate the auditory brain to suppress tinnitus.

The second set of limitations relates to the ICC location trends observed in our study. Differences exist in the number of modulated sites per ICC lamina with maximum modulation occurring in the middle frequency layer. Based on previous anatomical studies, there does not seem to be a differential pattern of excitatory and inhibitory synapses across

laminae that would suggest greater modulatory effects particularly for middle frequency regions (González-Hernández *et al.*, 1996; Nakamoto *et al.*, 2013; Saint Marie, 1996). The differential modulation seen across laminae may be due to the acoustic levels used in these experiments. In guinea pigs, auditory thresholds are lowest around 8 kHz (Gourevitch *et al.*, 2009; Heffner *et al.*, 1971), which coincides with our middle frequency lamina (i.e., 6.0-9.1 kHz). Thus, the chosen acoustic levels elicited stronger activity within the middle frequency lamina compared to the lower and higher frequency laminae, which may have enabled stronger modulation.

In terms of spatial trends within a given ICC lamina, there appears to be a random distribution of modulated and unmodulated sites. It is possible that we missed a location trend across the ICC due to insufficient mapping across each lamina per animal or even the use of multi-unit recordings. Individual neurons recorded on the same electrode site may have exhibited different modulation effects but the summation of their neural activity in the multi-unit recordings could have canceled out or masked these individual effects.

Stimulus timing dependent plasticity

The results presented in figure 9 suggest that the type and extent of modulation depends on the relative timing between paired acoustic-electrical stimulation. In particular, PAES-18 resulted in significantly more residual suppression and less residual facilitation than PAES-8. Both PAES-8 and ES-only exhibited similar amounts of residual spread for suppression and facilitation, whereas PAES-18 exhibited significantly greater residual spread of suppression than facilitation. This stimulus timing dependent plasticity can be likened to spike timing dependent plasticity; however, instead of looking at how pre- and post-synaptic cells potentiate or depress based on timing, we are looking at how electrical and acoustic stimulation facilitate or suppress a population of cells based on timing (Abbott and Nelson, 2000; Bi and Poo, 1998; Caporale and Dan, 2008; Dan and Poo, 2004; Magee and Johnston, 1997; Markram *et al.*, 1997; Yao and Dan, 2001; Zhang *et al.*, 1998). Spike and stimulus timing dependent plasticity have been demonstrated in the auditory system at the brainstem level as well as the cortex (Basura *et al.*, 2013; Dahmen *et al.*, 2008; Koehler and Shore, 2013b, a; Tzounopoulos *et al.*, 2004). Our results suggest that timing dependent plasticity induced by paired acoustic-electrical stimulation is also occurring at the auditory midbrain level. For PAES-18, the ICD-induced activity would have generally reached the ICC after the onset of acoustic-driven activity, which may have caused the stronger suppressive effect. A delay shorter than the 8 ms that was used for PAES-8 may have been needed for the ICD-induced activity to reach the ICC before the acoustic-driven activity to cause a stronger facilitatory effect. We did not observe any significant differences in facilitatory versus suppressive effects for PAES-8.

Two aspects of our protocol need to be considered when interpreting these results. First, we used a set ordering of the different stimulation paradigms with limited recovery time. We cannot rule out that the stronger suppressive effects caused by PAES-18 compared to PAES-8 or ES-only were partly attributed to the order and prolonged influence of the different stimulation paradigms. It may be possible that while ES-only did not result in large amounts of suppression, it did act as a primer allowing for larger suppression to occur in

response to PAES-18. Thus, the greater suppression seen following PAES-18 may be due to an individual paradigm or to the sequence of paradigms. At the same time, it may be possible that because of the large suppression occurring due to PAES-18, further suppression in response to PAES-8 was not possible. From our protocol and data, we can claim that it is possible to induce varying extents of suppressive versus facilitatory modulation, but whether it can be sufficiently achieved using a paired paradigm with a specific delay (e.g., PAES-18) or requires a sequence of stimulation paradigms (e.g., ES-only followed by PAES-18) warrants further investigation. For this initial study, we chose to focus on varying ICD and ICC electrode array placements with limited recovery time for several reasons explained in *Methods: Stimulation parameters*. This limited recovery makes it difficult to completely separate out the individual paradigm effects. Further studies are underway to parse out the modulatory effects that can be achieved by individual paradigms. For these studies, the ICC is probed with a repeated sequence of acoustic-only stimulation following each electrical stimulation paradigm in order to monitor the modulatory effects over time and to allow the effects to diminish before moving onto the next paradigm. Additionally, the stimulation site is held constant and each paradigm is presented in a random sequence throughout an experiment to further minimize any residual effects of one paradigm on another.

The second consideration in interpreting our plasticity results is that these experiments were performed under ketamine anesthesia, which may have influenced the types of modulatory effects observed in our study. Ketamine is known to influence auditory responses in the cortex (Gaese and Ostwald, 2001; Kisley and Gerstein, 1999; Syka *et al.*, 2005; Zurita *et al.*, 1994). In comparison, ketamine has been shown to have little or no effect on auditory coding within the ICC (Astl *et al.*, 1996; Ter-Mikaelian *et al.*, 2007). Ketamine may also limit plasticity changes in the auditory brain by effecting synaptic potentiation and depression (Leong *et al.*, 2004; Salami *et al.*, 2000). In this experiment, under ketamine anesthesia, we were still able to induce a significant amount of immediate and residual suppression and facilitation across the ICC with ICD stimulation. Therefore, we can conclude that the results are promising for eliciting differential modulation of neural activity across the ICC, but modulation by different paradigms needs to be verified in an awake preparation.

Clinical implications for tinnitus treatment

Tinnitus has commonly been associated with properties such as hyperactivity of neurons across the auditory system, including the ICC (Bauer *et al.*, 2008; Kaltenbach *et al.*, 2005; Lanting *et al.*, 2009; Ma *et al.*, 2006; Manzoor *et al.*, 2013; Melcher *et al.*, 2009; Møller, 2011; Mulders *et al.*, 2014; Norena and Eggermont, 2003; Roberts *et al.*, 2010; Vogler *et al.*, 2014). Based on the findings from this study, targeted ICD stimulation combined with varying delays of broadband noise stimulation may suppress activity in the ICC associated with tinnitus. Specifically, we found that using paired acoustic-electrical stimulation with a specific delay (i.e., PAES-18, though it may require a sequence of stimulation where ES-only precedes PAES-18) and stimulation of more medial and rostral ICD regions resulted in greater suppressive versus facilitatory effects in the ICC. Tinnitus has also been linked with other neural properties, such as hypersynchrony, tonotopic reorganization, and changes in

firing patterns, and within other auditory and non-auditory nuclei (Chen and Jastreboff, 1995; Chen *et al.*, 2012; Eggermont and Roberts, 2004; Galazyuk *et al.*, 2012; Komiya and Eggermont, 2000; Lockwood *et al.*, 1998; Møller, 1984; Muhlnickel *et al.*, 1998; Seki and Eggermont, 2003; Wienbruch *et al.*, 2006; Zhang *et al.*, 2003). We will need to investigate these neural properties, especially in tinnitus animal models, to assess if ICD stimulation can suppress or fix the pathogenic activity directly driving the tinnitus percept. Additionally, this treatment may also be relevant for a hyperacusis, a condition resulting in increased sensitivity to certain frequencies. We will need to determine if ICD stimulation can suppress the increased acoustic-driven activity and gain experienced and reduce sensitivity (Aazh *et al.*, 2014; Gu *et al.*, 2010). As discussed above, ICD stimulation may be activating passing fibers, such as from the contralateral IC, in addition to neurons projecting to the ICC from the ICD. Regardless of what is being activated, the main clinical goal would be to identify appropriate locations for array implantation and stimulation strategies that can induce neural changes that translate into therapeutic results for the patient.

There is already an ongoing clinical trial funded by the National Institutes of Health in which deaf patients will be implanted with the AMI. Many of these patients will also have tinnitus and can be stimulated with different electrode sites to evaluate their modulatory effects on the tinnitus percept. Based on our animal findings, we have decided to incorporate some of the stimulation paradigms into the clinical trial for treating tinnitus with the AMI. Before implantation, the AMI array needs to be modified to enable ICD simulation. Each AMI shank has a Dacron mesh that prevents over-insertion of the neuroprosthetic array into the IC and positions the sites within the ICC. To allow some sites to be placed in the ICD, each AMI shank will be modified to add dorsal sites closer to that mesh. With the initial AMI patient population, we will not be able to combine broadband noise stimulation with ICD stimulation since the patients will be deaf. However for these patients, we will investigate stimulation strategies that combine ICD stimulation with precisely timed stimulation across multiple ICC sites to attempt to mimic the paradigms used here as well as test the safety of this treatment. We will also not be able to access multiple locations throughout the ICD in human as was possible in our animal studies. As a results, electrodes may be implanted outside the optimal rostral and medial regions of ICD that appear to cause greater suppressive versus facilitatory effects. While our data shows that stimulation of different ICD locations generally modulates different subsets of ICC neurons, tinnitus treatment may then be limited if the electrode is not stimulating appropriate locations to target tinnitus-affected neurons. Since patients will already be implanted with the AMI for hearing restoration, we have the opportunity to investigate a wide range of stimulation patterns as best we can considering these limitations, which will hopefully reveal some parameters that can effectively suppress or at least modulate the tinnitus.

Demonstrating the ability to decrease the tinnitus percept in these initial AMI patients using paired ICD/ICC stimulation along with the suppression results from paired acoustic-electrical paradigms in animal studies could open up the possibility for implanting the AMI array in a larger population of patients with severe tinnitus. We would eventually seek a Phase I safety study for the treatment of tinnitus in patients with functional hearing in whom we can implement the paired acoustic-electrical stimulation paradigm. For patients who do

not have sufficient hearing, cochlear implants will remain an option that have been effective in reducing the tinnitus percept in some patient groups (Baguley and Atlas, 2007; Kleinjung *et al.*, 2009; Osaki *et al.*, 2005; Quaranta *et al.*, 2008; Van de Heyning *et al.*, 2008; Zeng *et al.*, 2011). Another possible alternative for patients with severe tinnitus with or without sufficient hearing is round window stimulation. Reduction in tinnitus using round window stimulation has been promising in acute cases (Portmann *et al.*, 1979; Cazals *et al.*, 1978; Rubinstein *et al.*, 2003), but repeatability of tinnitus suppression needs to be further explored (Møller, 2011; Punte *et al.*, 2013). More invasive approaches for treating tinnitus are being developed and increasingly used across different patient groups including stimulation of the auditory cortex or caudate nucleus as well as vagal nerve stimulation paired with acoustic stimulation (Cheung and Larson, 2010; De Ridder *et al.*, 2011; De Ridder *et al.*, 2014; Engineer *et al.*, 2011). While cochlear implants, round window stimulation, and several invasive brain treatments remain an option for some tinnitus patients, new approaches including AMI stimulation need to continually be developed so a larger population of patients can achieve tinnitus suppression.

Acknowledgments

References

Aazh H, McFerran D, Salvi R, Prasher D, Jastreboff M, Jastreboff P. Insights from the First International Conference on Hyperacusis: causes, evaluation, diagnosis and treatment. Noise Health. 2014; 16:123–6. [PubMed: 24804717]

Abbott LF, Nelson SB. Synaptic plasticity: taming the beast. Nat Neurosci. 2000; 3(Suppl):1178–83. [PubMed: 11127835]

Adams JC. Ascending projections to the inferior colliculus. J Comp Neurol. 1979; 183:519–38. [PubMed: 759446]

Aitkin LM, Dickhaus H, Schult W, Zimmermann M. External nucleus of inferior colliculus: auditory and spinal somatosensory afferents and their interactions. J Neurophysiol. 1978; 41:837–47. [PubMed: 681989]

Aitkin LM, Kenyon CE, Philpott P. The representation of the auditory and somatosensory systems in the external nucleus of the cat inferior colliculus. J Comp Neurol. 1981; 196:25–40. [PubMed: 7204665]

Aitkin LM, Phillips SC. Is the inferior colliculus an obligatory relay in the cat auditory system? Neurosci Lett. 1984a; 44:259–64. [PubMed: 6728296]

Aitkin LM, Phillips SC. The interconnections of the inferior colliculi through their commissure. J Comp Neurol. 1984b; 228:210–6. [PubMed: 6480913]

Astl J, Popelar J, Kvasnak E, Syka J. Comparison of response properties of neurons in the inferior colliculus of guinea pigs under different anesthetics. Audiology. 1996; 35:335–45. [PubMed: 9018367]

Baguley DM, Atlas MD. Cochlear implants and tinnitus. Prog Brain Res. 2007; 166:347–55. [PubMed: 17956799]

Bajo VM, King AJ. Cortical modulation of auditory processing in the midbrain. Front Neural Circuits. 2012; 6:114. [PubMed: 23316140]

Bajo VM, Moore DR. Descending projections from the auditory cortex to the inferior colliculus in the gerbil, Meriones unguiculatus. J Comp Neurol. 2005; 486:101–16. [PubMed: 15844210]

Bajo VM, Nodal FR, Bizley JK, Moore DR, King AJ. The ferret auditory cortex: descending projections to the inferior colliculus. Cereb Cortex. 2007; 17:475–91. [PubMed: 16581982]

Basura GJ, Koehler SD, Wiler JA, Shore SE. Multi-sensory integration in primary auditory cortex is stimulus timing dependent and alters neural synchrony. Assoc Res Otolaryng Abstr. 2013; 36:462.

Bauer CA, Turner JG, Caspary DM, Myers KS, Brozoski TJ. Tinnitus and inferior colliculus activity in chinchillas related to three distinct patterns of cochlear trauma. Journal of neuroscience research. 2008; 86:2564–78. [PubMed: 18438941]

Bi GQ, Poo MM. Synaptic modifications in cultured hippocampal neurons: dependence on spike timing, synaptic strength, and postsynaptic cell type. J Neurosci. 1998; 18:10464–72. [PubMed: 9852584]

Binns KE, Grant S, Withington DJ, Keating MJ. A topographic representation of auditory space in the external nucleus of the inferior colliculus of the guinea-pig. Brain Res. 1992; 589:231–42. [PubMed: 1393591]

Brozoski TJ, Bauer CA, Caspary DM. Elevated fusiform cell activity in the dorsal cochlear nucleus of chinchillas with psychophysical evidence of tinnitus. J Neurosci. 2002; 22:2383–90. [PubMed: 11896177]

Brunso-Bechtold JK, Thompson GC, Masterton RB. HRP study of the organization of auditory afferents ascending to central nucleus of inferior colliculus in cat. J Comp Neurol. 1981; 197:705–22. [PubMed: 7229134]

Caicedo A, Herbert H. Topography of descending projections from the inferior colliculus to auditory brainstem nuclei in the rat. J Comp Neurol. 1993; 328:377–92. [PubMed: 7680052]

Cant NB, Benson CG. Organization of the inferior colliculus of the gerbil (Meriones unguiculatus): differences in distribution of projections from the cochlear nuclei and the superior olivary complex. J Comp Neurol. 2006; 495:511–28. [PubMed: 16498677]

Caporale N, Dan Y. Spike timing-dependent plasticity: a Hebbian learning rule. Annu Rev Neurosci. 2008; 31:25–46. [PubMed: 18275283]

Casseday, JH.; Fremouw, T.; Covey, E. Springer Handbook of Auditory Research: Integrative Functions in the Mammalian Auditory Pathway. Oertel, D., et al., editors. Vol. 15. Springer-Verlag; New York: 2002. p. 238-318.

Cazals Y, Negrevergne M, Aran JM. Electrical stimulation of the cochlea in man: hearing induction and tinnitus suppression. J Am Audiol Soc. 1978; 3:209–13. [PubMed: 306987]

Chen GD, Jastreboff PJ. Salicylate-induced abnormal activity in the inferior colliculus of rats. Hear Res. 1995; 82:158–78. [PubMed: 7775282]

Chen GD, Manohar S, Salvi R. Amygdala hyperactivity and tonotopic shift after salicylate exposure. Brain Res. 2012; 1485:63–76. [PubMed: 22464181]

Cheung SW, Larson PS. Tinnitus modulation by deep brain stimulation in locus of caudate neurons (area LC). Neuroscience. 2010; 169:1768–78. [PubMed: 20541595]

Coleman JR, Clerici WJ. Sources of projections to subdivisions of the inferior colliculus in the rat. J Comp Neurol. 1987; 262:215–26. [PubMed: 3624552]

Colletti V, Shannon RV, Carner M, Veronese S, Colletti L. Progress in restoration of hearing with the auditory brainstem implant. Prog Brain Res. 2009; 175:333–45. [PubMed: 19660666]

Dahmen JC, Hartley DE, King AJ. Stimulus-timing-dependent plasticity of cortical frequency representation. J Neurosci. 2008; 28:13629–39. [PubMed: 19074036]

Dan Y, Poo MM. Spike timing-dependent plasticity of neural circuits. Neuron. 2004; 44:23–30. [PubMed: 15450157]

De Ridder D, Vanneste S, Engineer ND, Kilgard MP. Safety and efficacy of vagus nerve stimulation paired with tones for the treatment of tinnitus: a case series. Neuromodulation. 2014; 17:170–9. [PubMed: 24255953]

De Ridder D, Vanneste S, Kovacs S, Sunaert S, Menovsky T, van de Heyning P, Moller A. Transcranial magnetic stimulation and extradural electrodes implanted on secondary auditory cortex for tinnitus suppression. J Neurosurg. 2011; 114:903–11. [PubMed: 21235318]

Eggermont JJ, Kenmochi M. Salicylate and quinine selectively increase spontaneous firing rates in secondary auditory cortex. Hear Res. 1998; 117:149–60. [PubMed: 9557985]

Eggermont JJ, Roberts LE. The neuroscience of tinnitus Trends. Neurosci. 2004; 27:676–82.

Engineer ND, Riley JR, Seale JD, Vrana WA, Shetake JA, Sudanagunta SP, Borland MS, Kilgard MP. Reversing pathological neural activity using targeted plasticity. Nature. 2011; 470:101–4. [PubMed: 21228773]

Faye-Lund H. The neocortical projection to the inferior colliculus in the albino rat. Anat Embryol (Berl). 1985; 173:53–70. [PubMed: 2416247]

Faye-Lund H, Osen KK. Anatomy of the inferior colliculus in rat. Anat Embryol (Berl). 1985; 171:1–20. [PubMed: 3985354]

Feliciano M, Potashner SJ. Evidence for a glutamatergic pathway from the guinea pig auditory cortex to the inferior colliculus. J Neurochem. 1995; 65:1348–57. [PubMed: 7643112]

Gaese BH, Ostwald J. Anesthesia changes frequency tuning of neurons in the rat primary auditory cortex. J Neurophysiol. 2001; 86:1062–6. [PubMed: 11495976]

Galazyuk AV, Wenstrup JJ, Hamid MA. Tinnitus and underlying brain mechanisms. Curr Opin Otolaryngol Head Neck Surg. 2012; 20:409–15. [PubMed: 22931904]

Gao E, Suga N. Experience-dependent corticofugal adjustment of midbrain frequency map in bat auditory system. Proc Natl Acad Sci U S A. 1998; 95:12663–70. [PubMed: 9770543]

González Hernández TH, Meyer G, Ferres-Torres R. The commissural interconnections of the inferior colliculus in the albino mouse. Brain Res. 1986; 368:268–76. [PubMed: 2421840]

González-Hernández T, Mantolán-Sarmiento B, González-González B, Pérez-González H. Sources of GABAergic input to the inferior colliculus of the rat. J Comp Neurol. 1996; 372:309–26. [PubMed: 8863133]

Gourevitch B, Doisy T, Avillac M, Edeline JM. Follow-up of latency and threshold shifts of auditory brainstem responses after single and interrupted acoustic trauma in guinea pig. Brain Res. 2009; 1304:66–79. [PubMed: 19766602]

Green, D.; Swets, J. Signal Detection Theory and Psychophysics. Wiley; New York: 1966.

Gruters KG, Groh JM. Sounds and beyond: multisensory and other non-auditory signals in the inferior colliculus. Front Neural Circuits. 2012; 6:96. [PubMed: 23248584]

Gu JW, Halpin CF, Nam EC, Levine RA, Melcher JR. Tinnitus, diminished sound-level tolerance, and elevated auditory activity in humans with clinically normal hearing sensitivity. J Neurophysiol. 2010; 104:3361–70. [PubMed: 20881196]

Heffner R, Heffner H, Masterton B. Behavioral measurements of absolute and frequency-difference thresholds in guinea pig. J Acoust Soc Am. 1971; 49:1888–95. [PubMed: 5125738]

Herbert H, Aschoff A, Ostwald J. Topography of projections from the auditory cortex to the inferior colliculus in the rat. J Comp Neurol. 1991; 304:103–22. [PubMed: 2016407]

Hernández O, Rees A, Malmierca MS. A GABAergic component in the commissure of the inferior colliculus in rat. Neuroreport. 2006; 17:1611–4. [PubMed: 17001278]

Huffman RF, Henson OW Jr. The descending auditory pathway and acousticomotor systems: connections with the inferior colliculus. Brain Res Brain Res Rev. 1990; 15:295–323. [PubMed: 2289088]

Jen PH, Sun X, Chen QC. An electrophysiological study of neural pathways for corticofugally inhibited neurons in the central nucleus of the inferior colliculus of the big brown bat, Eptesicus fuscus. Exp Brain Res. 2001; 137:292–302. [PubMed: 11355376]

Jen PH, Zhou X, Zhang J, Chen QC, Sun X. Brief and short-term corticofugal modulation of acoustic signal processing in the bat midbrain. Hear Res. 2002; 168:196–207. [PubMed: 12117521]

Ji W, Gao E, Suga N. Effects of acetylcholine and atropine on plasticity of central auditory neurons caused by conditioning in bats. J Neurophysiol. 2001; 86:211–25. [PubMed: 11431503]

Ji W, Suga N. Tone-specific and nonspecific plasticity of inferior colliculus elicited by pseudo-conditioning: role of acetylcholine and auditory and somatosensory cortices. J Neurophysiol. 2009; 102:941–52. [PubMed: 19474174]

Kaltenbach JA, Zhang J, Finlayson P. Tinnitus as a plastic phenomenon and its possible neural underpinnings in the dorsal cochlear nucleus. Hear Res. 2005; 206:200–26. [PubMed: 16081009]

Kilgard MP, Merzenich MM. Cortical map reorganization enabled by nucleus basalis activity. Science. 1998; 279:1714–8. [PubMed: 9497289]

Kisley MA, Gerstein GL. Trial-to-trial variability and state-dependent modulation of auditory-evoked responses in cortex. J Neurosci. 1999; 19:10451–60. [PubMed: 10575042]

Kleinjung T, Steffens T, Strutz J, Langguth B. Curing tinnitus with a Cochlear Implant in a patient with unilateral sudden deafness: a case report. Cases journal. 2009; 2:7462. [PubMed: 19829970]

Knudsen EI. Instructed learning in the auditory localization pathway of the barn owl. Nature. 2002; 417:322–8. [PubMed: 12015612]

Koehler SD, Shore SE. Stimulus timing-dependent plasticity in dorsal cochlear nucleus is altered in tinnitus. J Neurosci. 2013a; 33:19647–56. [PubMed: 24336728]

Koehler SD, Shore SE. Stimulus-timing dependent multisensory plasticity in the guinea pig dorsal cochlear nucleus. PloS one. 2013b; 8:e59828. [PubMed: 23527274]

Komiya H, Eggermont JJ. Spontaneous firing activity of cortical neurons in adult cats with reorganized tonotopic map following pure-tone trauma. Acta Otolaryngol. 2000; 120:750–6. [PubMed: 11099153]

Langner G, Schreiner C, Merzenich MM. Covariation of latency and temporal resolution in the inferior colliculus of the cat. Hear Res. 1987; 31:197–201. [PubMed: 3446676]

Lanting CP, de KleineE, van DijkP. Neural activity underlying tinnitus generation: results from PET and fMRI. Hear Res. 2009; 255:1–13. [PubMed: 19545617]

LeBeau FE, Malmierca MS, Rees A. Iontophoresis in vivo demonstrates a key role for GABA(A) and glycinergic inhibition in shaping frequency response areas in the inferior colliculus of guinea pig. J Neurosci. 2001; 21:7303–12. [PubMed: 11549740]

Lenarz T, Lim HH, Reuter G, Patrick JF, Lenarz M. The auditory midbrain implant: a new auditory prosthesis for neural deafness-concept and device description. Otol Neurotol. 2006; 27:838–43. [PubMed: 16936570]

Leong D, Puil E, Schwarz D. Ketamine blocks non-N-methyl-D-aspartate receptor channels attenuating glutamatergic transmission in the auditory cortex. Acta Otolaryngol. 2004; 124:454–8. [PubMed: 15224874]

Lim HH, Anderson DJ. Auditory cortical responses to electrical stimulation of the inferior colliculus: implications for an auditory midbrain implant. J Neurophysiol. 2006; 96:975–88. [PubMed: 16723413]

Lim HH, Anderson DJ. Antidromic activation reveals tonotopically organized projections from primary auditory cortex to the central nucleus of the inferior colliculus in guinea pig. J Neurophysiol. 2007; 97:1413–27. [PubMed: 17151230]

Lim, HH.; Lenarz, M.; Lenarz, T. Implantable Neural Prostheses 1: Devices and Applications. Zhou, D.; Greenbaum, E., editors. Springer Science+Business Media, LLC; New York: 2009a. p. 117-54.

Lim HH, Lenarz M, Lenarz T. Auditory midbrain implant: a review Trends in amplification. 2009b; 13:149–80.

Lockwood AH, Salvi RJ, Coad ML, Towsley ML, Wack DS, Murphy BW. The functional neuroanatomy of tinnitus: evidence for limbic system links and neural plasticity. Neurology. 1998; 50:114–20. [PubMed: 9443467]

Loftus WC, Bishop DC, Oliver DL. Differential patterns of inputs create functional zones in central nucleus of inferior colliculus. J Neurosci. 2010; 30:13396–408. [PubMed: 20926666]

Ma WL, Hidaka H, May BJ. Spontaneous activity in the inferior colliculus of CBA/J mice after manipulations that induce tinnitus. Hear Res. 2006; 212:9–21. [PubMed: 16307852]

Magee JC, Johnston D. A synaptically controlled, associative signal for Hebbian plasticity in hippocampal neurons. Science. 1997; 275:209–13. [PubMed: 8985013]

Malmierca, M.; Ryugo, D. The Auditory Cortex. Winer, JA.; Schreiner, CE., editors. Springer US; 2011. p. 189-208.

Malmierca MS, Blackstad TW, Osen KK, Karagulle T, Molowny RL. The central nucleus of the inferior colliculus in rat: a Golgi and computer reconstruction study of neuronal and laminar structure. J Comp Neurol. 1993; 333:1–27. [PubMed: 7688006]

Malmierca MS, Hernandez O, Falconi A, Lopez-Poveda EA, Merchan M, Rees A. The commissure of the inferior colliculus shapes frequency response areas in rat: an in vivo study using reversible blockade with microinjection of kynurenic acid. Exp Brain Res. 2003; 153:522–9. [PubMed: 14508633]

Malmierca MS, Hernandez O, Rees A. Intercollicular commissural projections modulate neuronal responses in the inferior colliculus. Eur J Neurosci. 2005; 21:2701–10. [PubMed: 15926918]

Malmierca MS, Izquierdo MA, Cristaudo S, Hernandez O, Perez-Gonzalez D, Covey E, Oliver DL. A discontinuous tonotopic organization in the inferior colliculus of the rat. J Neurosci. 2008; 28:4767–76. [PubMed: 18448653]

Malmierca MS, Rees A, Le Beau FE, Bjaalie JG. Laminar organization of frequency-defined local axons within and between the inferior colliculi of the guinea pig. J Comp Neurol. 1995; 357:124–44. [PubMed: 7673462]

Manzoor NF, Gao Y, Licari F, Kaltenbach JA. Comparison and contrast of noise-induced hyperactivity in the dorsal cochlear nucleus and inferior colliculus. Hear Res. 2013; 295:114–23. [PubMed: 22521905]

Markovitz CD, Tang TT, Edge DP, Lim HH. Three-dimensional brain reconstruction of in vivo electrode tracks for neuroscience and neural prosthetic applications. Frontiers in Neural Circuits. 2012; 6

Markovitz CD, Tang TT, Lim HH. Tonotopic and localized pathways from primary auditory cortex to the central nucleus of the inferior colliculus. Front Neural Circuits. 2013; 7:77. [PubMed: 23641201]

Markram H, Lübke J, Frotscher M, Sakmann B. Regulation of synaptic efficacy by coincidence of postsynaptic APs and EPSPs. Science. 1997; 275:213–5. [PubMed: 8985014]

McIntyre CC, Grill WM. Selective microstimulation of central nervous system neurons. Ann Biomed Eng. 2000; 28:219–33. [PubMed: 10784087]

Meininger V, Pol D, Derer P. The inferior colliculus of the mouse. A Nissl and Golgi study. Neuroscience. 1986; 17:1159–79. [PubMed: 2423921]

Melcher JR, Levine RA, Bergevin C, Norris B. The auditory midbrain of people with tinnitus: abnormal sound-evoked activity revisited. Hear Res. 2009; 257:63–74. [PubMed: 19699287]

Merzenich MM, Reid MD. Representation of the cochlea within the inferior colliculus of the cat. Brain Res. 1974; 77:397–415. [PubMed: 4854119]

Mitani A, Shimokouchi M, Nomura S. Effects of stimulation of the primary auditory cortex upon colliculogeniculate neurons in the inferior colliculus of the cat. Neurosci Lett. 1983; 42:185–9. [PubMed: 6664630]

Moore DR, Kotak VC, Sanes DH. Commissural and lemniscal synaptic input to the gerbil inferior colliculus. J Neurophysiol. 1998; 80:2229–36. [PubMed: 9819238]

Morest DK, Oliver DL. The neuronal architecture of the inferior colliculus in the cat: defining the functional anatomy of the auditory midbrain. J Comp Neurol. 1984; 222:209–36. [PubMed: 6699208]

Muhlnickel W, Elbert T, Taub E, Flor H. Reorganization of auditory cortex in tinnitus. Proc Natl Acad Sci U S A. 1998; 95:10340–3. [PubMed: 9707649]

Mulders WH, Barry KM, Robertson D. Effects of furosemide on cochlear neural activity, central hyperactivity and behavioural tinnitus after cochlear trauma in guinea pig. PLoS One. 2014; 9:e97948. [PubMed: 24835470]

Møller AR. Pathophysiology of tinnitus. Ann Otol Rhinol Laryngol. 1984; 93:39–44. [PubMed: 6367601]

Møller, AR.; Langguth, B.; DeRidder, D.; Kleinjung, T., editors. Textbook of tinnitus. Springer Science+Business Media, LLC; New York: 2011.

Nakamoto KT, Jones SJ, Palmer AR. Descending projections from auditory cortex modulate sensitivity in the midbrain to cues for spatial position. J Neurophysiol. 2008; 99:2347–56. [PubMed: 18385487]

Nakamoto KT, Mellott JG, Killius J, Storey-Workley ME, Sowick CS, Schofield BR. Analysis of excitatory synapses in the guinea pig inferior colliculus: a study using electron microscopy and GABA immunocytochemistry. Neuroscience. 2013; 237:170–83. [PubMed: 23395860]

Norena AJ, Eggermont JJ. Changes in spontaneous neural activity immediately after an acoustic trauma: implications for neural correlates of tinnitus. Hear Res. 2003; 183:137–53. [PubMed: 13679145]

Oliver, DL. The Inferior Colliculus. Winer, JA.; Schreiner, CE., editors. Springer Science+Business Media, Inc.; New York: 2005. p. 69-114.

Oliver DL, Beckius GE, Shneiderman A. Axonal projections from the lateral and medial superior olive to the inferior colliculus of the cat: a study using electron microscopic autoradiography. J Comp Neurol. 1995; 360:17–32. [PubMed: 7499562]

Oliver DL, Morest DK. The central nucleus of the inferior colliculus in the cat. J Comp Neurol. 1984; 222:237–64. [PubMed: 6699209]

Osaki Y, Nishimura H, Takasawa M, Imaizumi M, Kawashima T, Iwaki T, Oku N, Hashikawa K, Doi K, Nishimura T, Hatazawa J, Kubo T. Neural mechanism of residual inhibition of tinnitus in cochlear implant users. Neuroreport. 2005; 16:1625–8. [PubMed: 16189467]

Palmer AR, Shackleton TM, Sumner CJ, Zobay O, Rees A. Classification of frequency response areas in the inferior colliculus reveals continua not discrete classes. J Physiol. 2013; 591:4003–25. [PubMed: 23753527]

Portmann M, Cazals Y, Negrevergne M, Aran JM. Temporary tinnitus suppression in man through electrical stimulation of the cochlea. Acta Otolaryngol. 1979; 87:294–9. [PubMed: 312586]

Punte AK, De Ridder D, Van de Heyning P. On the necessity of full length electrical cochlear stimulation to suppress severe tinnitus in single-sided deafness. Hear Res. 2013; 295:24–9. [PubMed: 23418635]

Quaranta N, Fernandez-Vega S, D'elia C, Filipo R, Quaranta A. The effect of unilateral multichannel cochlear implant on bilaterally perceived tinnitus. Acta Otolaryngol. 2008; 128:159–63. [PubMed: 17851950]

Ranck JB Jr. Which elements are excited in electrical stimulation of mammalian central nervous system: a review. Brain Res. 1975; 98:417–40. [PubMed: 1102064]

Roberts LE, Eggermont JJ, Caspary DM, Shore SE, Melcher JR, Kaltenbach JA. Ringing ears: the neuroscience of tinnitus. J Neurosci. 2010; 30:14972–9. [PubMed: 21068300]

Rockel AJ, Jones EG. The neuronal organization of the inferior colliculus of the adult cat. I. The central nucleus J Comp Neurol. 1973; 147:11–60.

Roth GL, Aitkin LM, Andersen RA, Merzenich MM. Some features of the spatial organization of the central nucleus of the inferior colliculus of the cat. J Comp Neurol. 1978; 182:661–80. [PubMed: 721973]

Rubinstein JT, Tyler RS, Johnson A, Brown CJ. Electrical suppression of tinnitus with high-rate pulse trains. Otol Neurotol. 2003; 24:478–85. [PubMed: 12806303]

Ruxton GD. The unequal variance t-test is an underused alternative to the Student's t-test and the Mann-Whitney U test. Behav Ecol. 2006; 17:688–90.

Saint Marie RL. Glutamatergic connections of the auditory midbrain: selective uptake and axonal transport of D-[3H]aspartate. J Comp Neurol. 1996; 373:255–70. [PubMed: 8889926]

Saint Marie RL, Baker RA. Neurotransmitter-specific uptake and retrograde transport of [3H]glycine from the inferior colliculus by ipsilateral projections of the superior olivary complex and nuclei of the lateral lemniscus. Brain Res. 1990; 524:244–53. [PubMed: 1705464]

Salami M, Fathollahi Y, Esteky H, Motamedi F, Atapour N. Effects of ketamine on synaptic transmission and long-term potentiation in layer II/III of rat visual cortex in vitro. Eur J Pharmacol. 2000; 390:287–93. [PubMed: 10708735]

Saldana E, Feliciano M, Mugnaini E. Distribution of descending projections from primary auditory neocortex to inferior colliculus mimics the topography of intracollicular projections. J Comp Neurol. 1996; 371:15–40. [PubMed: 8835717]

Saldana, E.; Merchan, MA. The Inferior Colliculus. Winer, JA.; Schreiner, CE., editors. Springer Science+Business Media, Inc.; New York: 2005. p. 155-81.

Saldaña E, Merchán MA. Intrinsic and commissural connections of the rat inferior colliculus. J Comp Neurol. 1992; 319:417–37. [PubMed: 1376335]

Samii A, Lenarz M, Majdani O, Lim HH, Samii M, Lenarz T. Auditory midbrain implant: a combined approach for vestibular schwannoma surgery and device implantation. Otol Neurotol. 2007; 28:31–8. [PubMed: 17195743]

Schofield BR, Cant NB. Projections from the ventral cochlear nucleus to the inferior colliculus and the contralateral cochlear nucleus in guinea pigs. Hear Res. 1996; 102:1–14. [PubMed: 8951445]

Schreiner CE, Langner G. Periodicity coding in the inferior colliculus of the cat. II. Topographical organization. J Neurophysiol. 1988; 60:1823–40. [PubMed: 3236053]

Schwartz MS, Otto SR, Shannon RV, Hitselberger WE, Brackmann DE. Auditory brainstem implants. Neurotherapeutics. 2008; 5:128–36. [PubMed: 18164492]

Seki S, Eggermont JJ. Changes in spontaneous firing rate and neural synchrony in cat primary auditory cortex after localized tone-induced hearing loss. Hear Res. 2003; 180:28–38. [PubMed: 12782350]

Shneiderman A, Oliver DL, Henkel CK. Connections of the dorsal nucleus of the lateral lemniscus: an inhibitory parallel pathway in the ascending auditory system? J Comp Neurol. 1988; 276:188–208. [PubMed: 3220980]

Smith PH. Anatomy and physiology of multipolar cells in the rat inferior collicular cortex using the in vitro brain slice technique. J Neurosci. 1992; 12:3700–15. [PubMed: 1356146]

Snyder RL, Bierer JA, Middlebrooks JC. Topographic spread of inferior colliculus activation in response to acoustic and intracochlear electric stimulation. J Assoc Res Otolaryngol. 2004; 5:305–22. [PubMed: 15492888]

Straka M, Schendel D, Lim HH. Neural integration and enhancement from the inferior colliculus up to different layers of auditory cortex. J Neurophysiol. 2013

Straka MM, McMahon M, Markovitz CD, Lim HH. Effects of location and timing of co-activated neurons in the auditory midbrain on cortical activity: implications for a new central auditory prosthesis. J Neural Eng. 2014; 11:046021. [PubMed: 25003629]

Suga N, Ma X. Multiparametric corticofugal modulation and plasticity in the auditory system. Nat Rev Neurosci. 2003; 4:783–94. [PubMed: 14523378]

Sun XD, Jen PH, Sun DX, Zhang SF. Corticofugal influences on the responses of bat inferior collicular neurons to sound stimulation. Brain Res. 1989; 495:1–8. [PubMed: 2776027]

Syka J, Popelar J. Inferior colliculus in the rat: neuronal responses to stimulation of the auditory cortex. Neurosci Lett. 1984; 51:235–40. [PubMed: 6514239]

Syka J, Popelar J, Kvasnak E, Astl J. Response properties of neurons in the central nucleus and external and dorsal cortices of the inferior colliculus in guinea pig. Exp Brain Res. 2000; 133:254–66. [PubMed: 10968227]

Syka J, Suta D, Popelar J. Responses to species-specific vocalizations in the auditory cortex of awake and anesthetized guinea pigs. Hear Res. 2005; 206:177–84. [PubMed: 16081007]

Ter-Mikaelian M, Sanes DH, Semple MN. Transformation of temporal properties between auditory midbrain and cortex in the awake Mongolian gerbil. J Neurosci. 2007; 27:6091–102. [PubMed: 17553982]

Torterolo P, Zurita P, Pedemonte M, Velluti RA. Auditory cortical efferent actions upon inferior colliculus unitary activity in the guinea pig. Neurosci Lett. 1998; 249:172–6. [PubMed: 9682844]

Tzounopoulos T, Kim Y, Oertel D, Trussell LO. Cell-specific, spike timing-dependent plasticities in the dorsal cochlear nucleus. Nat Neurosci. 2004; 7:719–25. [PubMed: 15208632]

Van de Heyning P, Vermeire K, Diebl M, Nopp P, Anderson I, De RidderD. Incapacitating unilateral tinnitus in single-sided deafness treated by cochlear implantation. Ann Otol Rhinol Laryngol. 2008; 117:645–52. [PubMed: 18834065]

Vogler DP, Robertson D, Mulders WH. Hyperactivity following unilateral hearing loss in characterized cells in the inferior colliculus. Neuroscience. 2014

Wang H, Brozoski TJ, Caspary DM. Inhibitory neurotransmission in animal models of tinnitus: maladaptive plasticity. Hear Res. 2011; 279:111–7. [PubMed: 21527325]

Weinberger NM, Javid R, Lepan B. Long-term retention of learning-induced receptive-field plasticity in the auditory cortex. Proc Natl Acad Sci U S A. 1993; 90:2394–8. [PubMed: 8460150]

Wienbruch C, Paul I, Weisz N, Elbert T, Roberts LE. Frequency organization of the 40-Hz auditory steady-state response in normal hearing and in tinnitus. Neuroimage. 2006; 33:180–94. [PubMed: 16901722]

Winer JA, Larue DT, Diehl JJ, Hefti BJ. Auditory cortical projections to the cat inferior colliculus. J Comp Neurol. 1998; 400:147–74. [PubMed: 9766397]

Xiong Y, Zhang Y, Yan J. The neurobiology of sound-specific auditory plasticity: a core neural circuit. Neuroscience and biobehavioral reviews. 2009; 33:1178–84. [PubMed: 19014967]

Yan J, Ehret G. Corticofugal modulation of midbrain sound processing in the house mouse. Eur J Neurosci. 2002; 16:119–28. [PubMed: 12153536]

Yan J, Suga N. Corticofugal amplification of facilitative auditory responses of subcortical combination-sensitive neurons in the mustached bat. J Neurophysiol. 1999; 81:817–24. [PubMed: 10036282]

Yan W, Suga N. Corticofugal modulation of the midbrain frequency map in the bat auditory system. Nat Neurosci. 1998; 1:54–8. [PubMed: 10195109]

Yao H, Dan Y. Stimulus timing-dependent plasticity in cortical processing of orientation. Neuron. 2001; 32:315–23. [PubMed: 11684000]

Zeng FG, Tang Q, Dimitrijevic A, Starr A, Larky J, Blevins NH. Tinnitus suppression by low-rate electric stimulation and its electrophysiological mechanisms. Hear Res. 2011; 277:61–6. [PubMed: 21447376]

Zhang JS, Kaltenbach JA. Increases in spontaneous activity in the dorsal cochlear nucleus of the rat following exposure to high-intensity sound. Neurosci Lett. 1998; 250:197–200. [PubMed: 9708866]

Zhang JS, Kaltenbach JA, Wang J, Kim SA. Fos-like immunoreactivity in auditory and nonauditory brain structures of hamsters previously exposed to intense sound. 153. Exp Brain Res. 2003:655–60.

Zhang LI, Tao HW, Holt CE, Harris WA, Poo M. A critical window for cooperation and competition among developing retinotectal synapses. Nature. 1998; 395:37–44. [PubMed: 9738497]

Zhang Y, Suga N. Modulation of responses and frequency tuning of thalamic and collicular neurons by cortical activation in mustached bats. J Neurophysiol. 2000; 84:325–33. [PubMed: 10899207]

Zhang Y, Suga N, Yan J. Corticofugal modulation of frequency processing in bat auditory system. Nature. 1997; 387:900–3. [PubMed: 9202121]

Zhou X, Jen PH. Brief and short-term corticofugal modulation of subcortical auditory responses in the big brown bat, Eptesicus fuscus. J Neurophysiol. 2000; 84:3083–7. [PubMed: 11110836]

Zurita P, Villa AE, de Ribaupierre Y, de RibaupierreF, Rouiller EM. Changes of single unit activity in the cat's auditory thalamus and cortex associated to different anesthetic conditions. Neurosci Res. 1994; 19:303–16. [PubMed: 8058206]
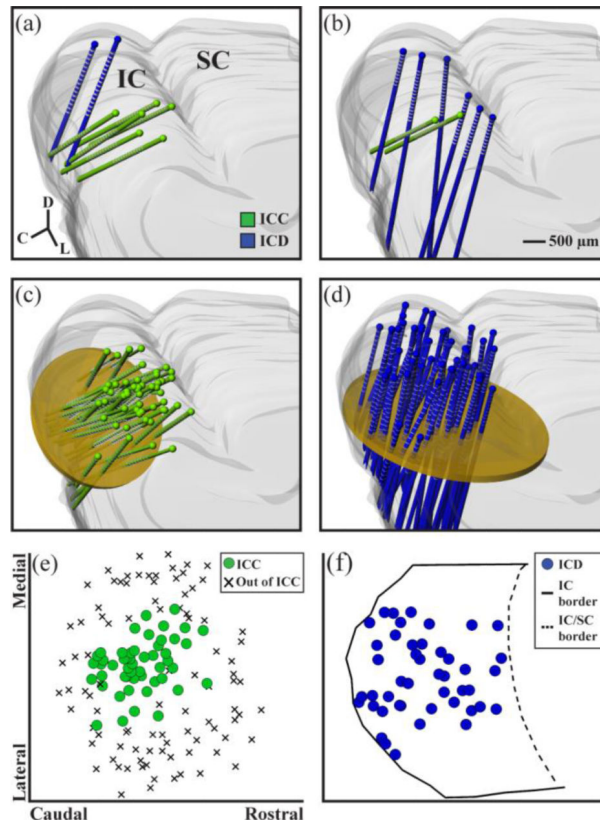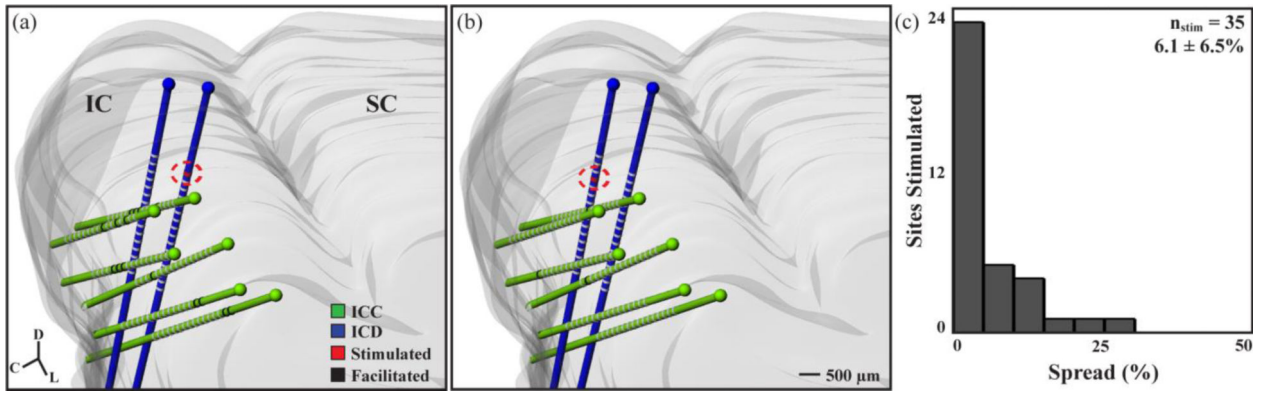
Figure 1.
Experimental protocols and array placements. In five experiments, one stimulation array placement (each array consists of two shanks) was made in the ICD and multiple recording array placements across the ICC (a). In seven experiments, one recording array placement was made in the ICC and multiple stimulating array placements in the ICD (b). All of the recording array placements (n=51 shanks shown in green) and all of the stimulating array placements (n=45 shanks shown in blue) were superimposed onto a single 3D reconstruction of the IC in (c) and (d), respectively. Planar cuts (shown in yellow) were made through the reconstructions orthogonal to the electrode array trajectories. Coordinates of the shanks through each plane are plotted as 2D maps in (e) and (f). For the recording locations in (e), each shank location was plotted along what is approximated as an isofrequency lamina that also includes recording locations identified as being outside of the ICC in order to show that we fully spanned the isofrequency dimension of the ICC. For the stimulation locations in (f), the borders of the IC were included on the horizontal plane in order to show that we fully spanned the rostral-caudal extent of the ICD. We were unable to sample the most medial portion of the ICD due to obstructive vasculature on the occipital cortex surface. The most lateral locations may include some portions of the ICX.
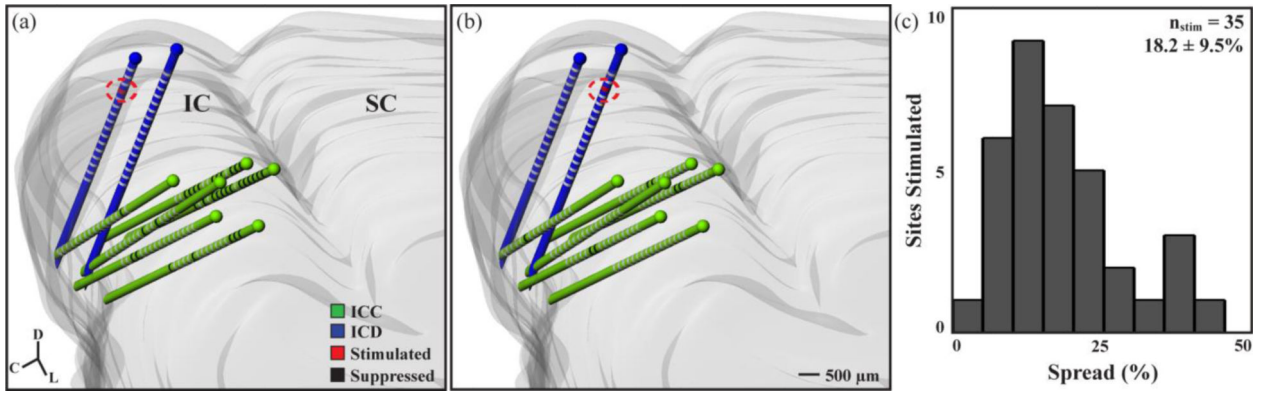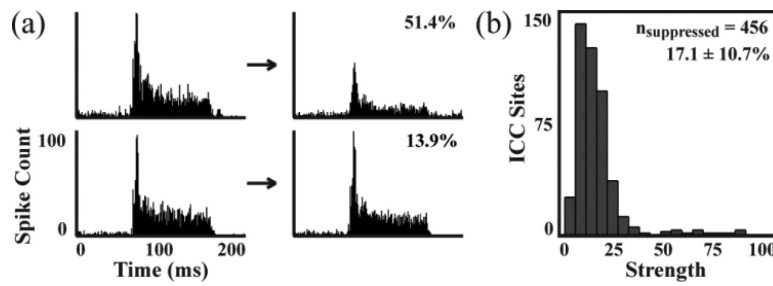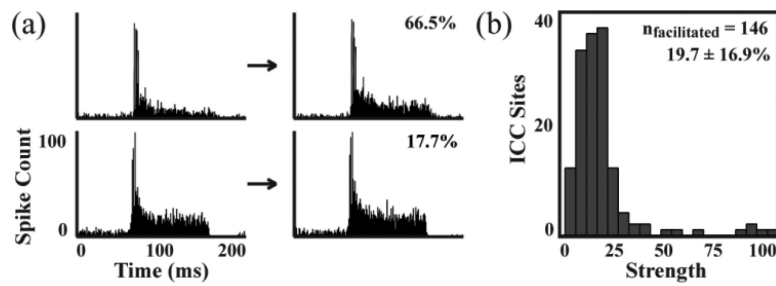
Figure 2.
Examples across cases show variability of suppression spread. A single stimulation site in the ICD (circled in red) resulted in a suppression spread of 46.0% (a - 29 significantly suppressed sites out of 63 ICC sites shown in black, see *Methods: Data Analysis* for statistical methods) compared to an ICD stimulation site 500 µm away that resulted in a suppression spread of 11.1% (b - 7 of 63 ICC sites). A histogram of the suppression spread resulting from 35 stimulated ICD sites from 5 animals is shown in (c) with an average of 18.2 ± 9.5% (mean ± SD). A total of 2428 ICC sites were included in this analysis, with 456 ICC sites showing suppression.

Figure 3.
Examples across cases show variability of facilitation spread. A single stimulation site in the ICD (circled in red) resulted in a facilitation spread of 23.4% (a - 15 significantly facilitated sites out of 64 ICC sites shown in black) while another ICD site 500 μm away resulted in a facilitation spread of 4.7% (b - 3 of 64 ICC sites). A histogram of the facilitation spread resulting from 35 stimulated ICD sites from 5 animals is shown in (c) with an average of 6.1 ± 6.5% (mean ± SD). A total of 2428 ICC sites were included in this analysis, with 146 ICC sites showing facilitation.

Figure 4.
Examples of suppression strength. Stimulation of a single ICD site could induce strong suppression (a - 51.4% decrease) or weak suppression (b- 13.9% decrease) on different ICC sites. A total of 456 out of 2428 ICC sites were suppressed by the 35 stimulated ICD sites from Fig. 2 and 3 with an average decrease of 17.1 ± 10.7% (c).
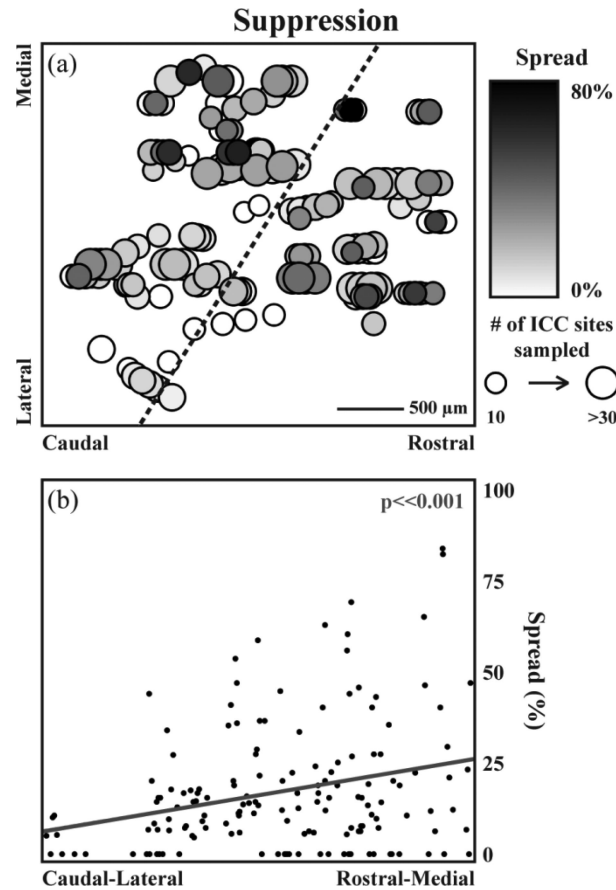
Figure 5.
Examples of facilitation strength. Stimulation of a single ICD site could induce strong
facilitation (a - 66.5% decrease) or weak facilitation (b - 17.7% decrease) on different ICC
sites. A total of 146 out of 2428 ICC sites were facilitated by the 35 stimulated ICD sites
from Fig. 2 and 3 with an average increase of 19.7 ± 16.9% (c).
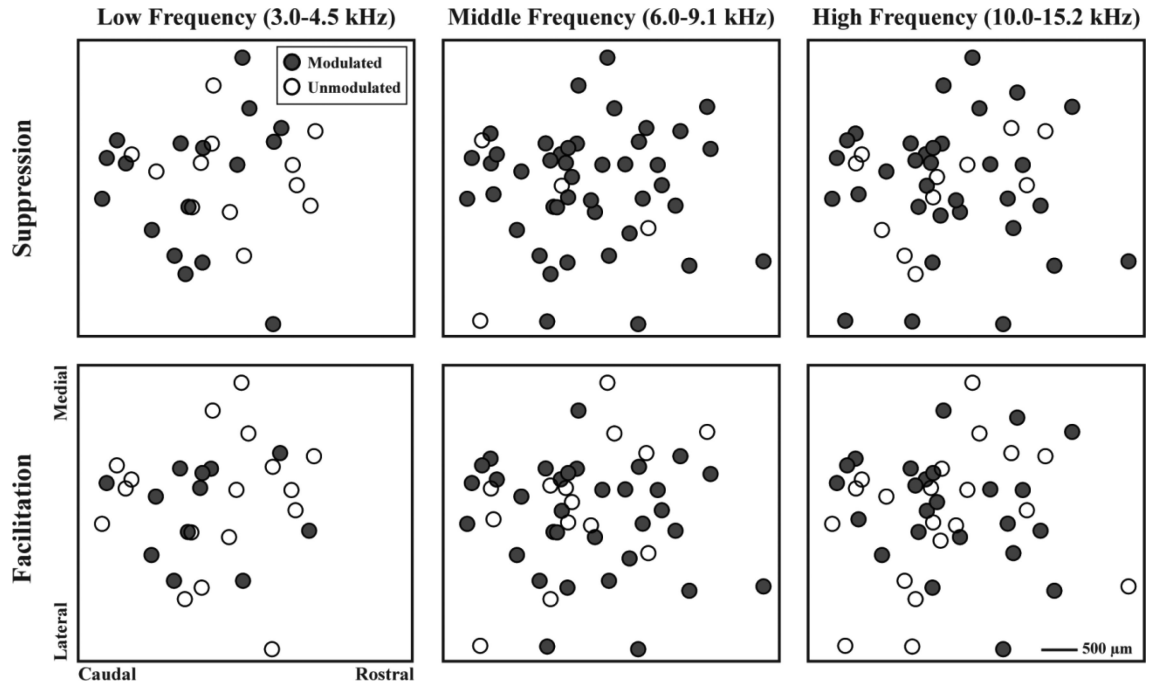
Figure 6.
Modulation across an ICC lamina. ICC recording sites from 12 animals and three different frequency ranges (low frequency, n_{shanks}=29, n_{sites}=86; middle frequency, n_{shanks}=47, n_{sites}=189; high frequency, n_{shanks}= 44, n_{sites}=158) were mapped onto their corresponding isofrequency plane. Modulated locations showed significant suppressive or facilitatory residual changes to PAES-18. Modulated and unmodulated locations were distributed throughout an entire ICC lamina.
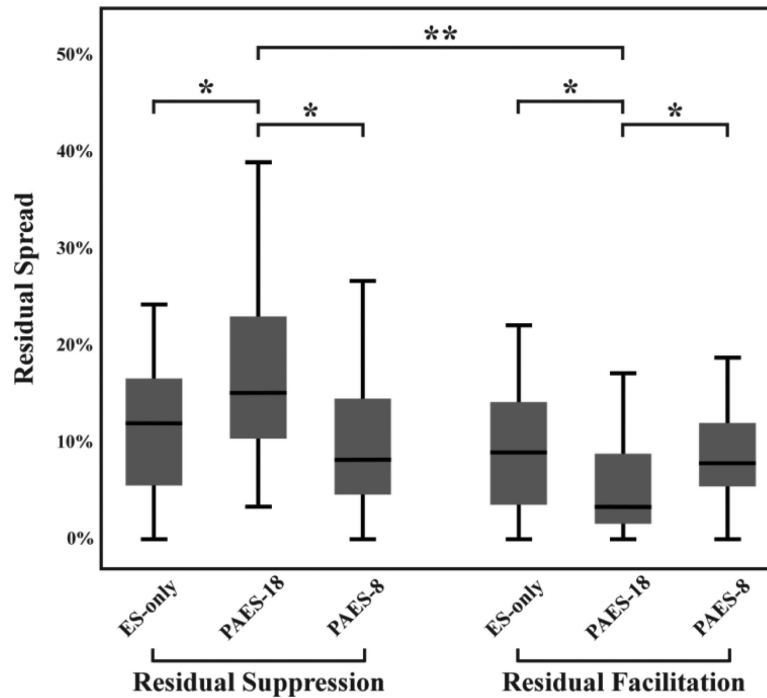
Figure 7.
Residual suppression spread depends on ICD stimulation location. All stimulation sites (n=154) were mapped onto a horizontal plane through the ICD (a). Two parameters were mapped along the plane: spread and total number of sites that could be modulated. Large-dark circles indicate that maximal suppressive spread across the ICC can be elicited by stimulation of that ICD location. The suppression spread significantly increased (p<<0.001) as a function of location along the steepest gradient axis from the caudal-lateral to the rostral-medial regions in the ICD (b). The steepest gradient axis for suppression spread is shown on the map in (a) as a dotted line. A total of 740 out of 4109 ICD-ICC site pairs were suppressed by ICD stimulation.
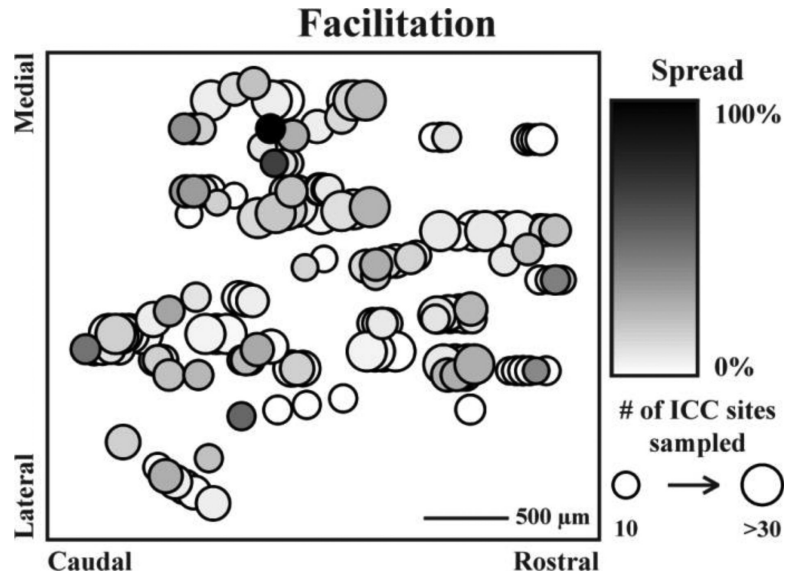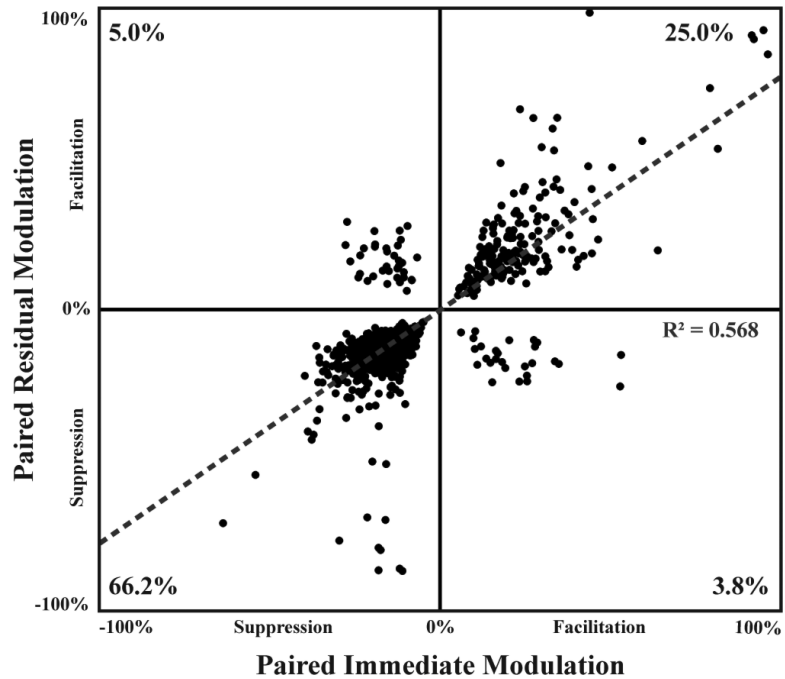
Figure 8.
No trend for ICD stimulation location was observed for residual facilitation spread. All stimulation sites (n=154) were mapped onto a horizontal plane through the ICD. Two parameters were mapped along the plane: spread and total number of sites that could be modulated. Large-dark circles indicate that maximal facilitatory spread across the ICC can be elicited by stimulation of that ICD location. A total of 314 out of 4109 ICD-ICC site pairs were facilitated by ICD stimulation.

Figure 9.
Comparison of residual spread induced by different stimulation paradigms. PAES-18 induced significantly more residual suppression and less residual facilitation than ES-only and PAES-8 (two-tailed, unequal variance, ranked t-test with Bonferroni correction; $p<0.05$ *). PAES-18 also induced significantly more suppression than facilitation ($p\ll0.001$ **). This figure plots the median and distribution of suppression and facilitation spread values. The mean ± SD for each paradigm are as follows: ES-only - suppression spread = $12.9 ± 8.9\%$ and facilitation spread = $9.9 ± 6.9\%$; PAES-18 - suppression spread = $18.2 ± 9.7\%$ and facilitation spread = $6.1 ± 6.5\%$; PAES-8 - suppression spread = $12.5 ± 12.1\%$ and facilitation spread = $9.6 ± 5.9\%$. The total number of ICC sites analyzed and the resulting number of sites suppressed and facilitated are as follows: ES-only 324 suppressed and 219 facilitated out of 2377 ICC sites; PAES-18 - 456 suppressed and 146 facilitated out of 2428 ICC sites; PAES-8 - 288 suppressed and 222 facilitated out of 2313 ICC sites.

Figure 10.
Type of immediate modulation generally directs the type of residual modulation. Sites that exhibited significant immediate and significant residual modulation due to a paired paradigm were plotted based on the strength of each of the modulations (n_{total}=705). Data was pooled from PAES-18 and PAES- 8 to assess the relationship between immediate and residual modulation regardless of the paired paradigm used. Immediate and residual modulations were typically in the same direction (i.e., both suppressive or both facilitatory) in which 66.2% of the sites were suppressed and 25% were facilitated. Only 8.8% of the sites showed a switch in modulation type.

Table 1

Immediate and residual modulation resulting from paired paradigms

Immediate Modulation	Residual Modulation	Number of ICD-ICC Site Pairs	Percentage
Suppression	Suppression	467	5.76
Facilitation	Facilitation	176	2.17
Suppression	Facilitation	35	0.43
Facilitation	Suppression	27	0.33
Suppression	No Change	690	8.52
Facilitation	No Change	481	5.94
No Change	Suppression	763	9.42
No Change	Facilitation	520	6.42
No Change	No Change	4943	61.01

ICD-ICC site pairs were pooled for this analysis from both PAES-18 and PAES-8 to determine if a correlation exists between immediate and residual modulation regardless of the paired paradigm used. A total of 8102 ICD-ICC site pairs showed significant immediate and/or residual modulation due to PAES-18 (4109 ICD-ICC site pairs) or PAES-8 (3993 ICD-ICC site pairs). Results show that 8.7% of all ICD-ICC site pairs are both immediately and residually modulated while 14.4% are only immediately modulated and 15.8% are only residually modulated due to paired paradigms.